AFOSR-TR- 94 0252

Multidisciplinary Studies of Integrated Neural Network Systems

Final Technical Report
December 1, 1989 - December 31, 1993

Contract No.: F49620-90-0010
ARPA Order: 7013
Program Code: 9D10
Effective Date of Contract: 12/1/89
Amount of Contract Dollars: 500K

John Pearson, Project Director
(609) 734-2385
David Sarnoff Research Center
Princeton, N.J. 08543-5300

March 1994

Sponsored by
Advanced Research Projects Agency
ARPA Order No. 7013
Monitored by AFOSR Under Contract No. F49620-90-C-0010

REPORT DOCUMENTATION PAGE

Form Approved
OMB No. 0704-0188

1. AGENCY USE ONLY *(Leave Blank)*	2. REPORT DATE	3. REPORT TYPE AND DATES COVERED
	March 1994	Final Report - 12/1/89 - 12/31/93

4. TITLE AND SUBTITLE

Multidisciplinary Studies of Integrated Neural Network Systems

5. FUNDING NUMBERS

F49620-90-C-0010
61101E
7013
10

6. AUTHOR(S)

John Pearson, Clay Spence, Williams E. Sullivan, Jeffrey Lubin, Jack Gelfand, Steven Lane, David Handelman, Mike Littman

7. PERFORMING ORGANIZATION NAME(S) AND ADDRESS(ES)

David Sarnoff Research Center
201 Washington Rd.
Princeton, NJ 08543-5300

Princeton University
Princeton, NJ 08540

ROBICON, Inc.
330 Alexander St.
Princeton, NJ 08540

8. PERFORMING ORGANIZATION REPORT NUMBER

AFOSR-TR- 94 0252

9. SPONSORING/MONITORING AGENCY NAME(S) AND ADDRESS(ES)

Defense Advanced Research Project Agency
Arlington, VA 22203-1714

AFOSR/NL
110 Duncan Ave, Suite B115
Bolling AFB, DC 20332-0001
DF Tangney

10. SPONSORING/MONITORING AGENCY REPORT NUMBER

11. SUPPLEMENTARY NOTES

12a. DISTRIBUTION/AVAILABILITY STATEMENT

Approved for public release;
distribution unlimited.

12. DISTRIBUTION CODE

13. ABSTRACT *(Maximum 200 words)*

This project was a joint effort of the David Sarnoff Research Center (Sarnoff), Princeton University, and Robicon Systems, all of Princeton, NJ. It consisted of three sub-projects, each concerned with a similar kind of research -- the development of artificial adaptive systems with capabilities similar to those of their biological counterparts. Recent work on neural networks has demonstrated their potential for solving difficult problems in simplified, controlled environments. The next stage in the development of neural networks is their extension to the scale, complexity, and variability of real-world situations. This will not be a simple evolution of existing neural net designs, because it requires the integration of complex adaptive systems whose components have widely differing functions. Fortunately, biological organisms present existing solutions to this problem and neuroscience can now probe in detail the relevant structures. Biological systems are highly adaptive and operate well in extremely complex and variable environments. They accomplish this by partitioning the system into functional sub-units in a quasi-hierarchical structure of neural network modules. We studied three specific examples of this system integration strategy and modeled their operation for the purpose of creating new neural network architectures and control schemes.

14. SUBJECT TERMS

Neural networks, auditory localization, sensor fusion, neuroscience, target detection, motion analysis, visual cortex, barn owl, robotics, expert systems, hierarchical architectures, adaptive control

15. NUMBER OF PAGES

34

16. PRICE CODE

17. SECURITY CLASSIFICATION OF REPORT	18. SECURITY CLASSIFICATION OF THIS PAGE	19. SECURITY CLASSIFICATION OF ABSTRACT	20. LIMITATION OF ABSTRACT
UNCLASSIFIED	UNCLASSIFIED	UNCLASSIFIED	200 words

TABLE OF CONTENTS

LIST OF FIGURES

Section I Self-Supervised Learning Within a System of Map-Like NeuralNetworks

Section II Modeling Adaptive Processing in the Visual Cortex

Section III Hierarchical Architectures and Integration of Neural Networks and Knowledge-Based Systems for Intelligent Robotic Control

Introduction

This project was a joint effort of the David Sarnoff Research Center (Sarnoff), Princeton University, and Robicon Systems, all of Princeton, NJ. It was a multi-disciplinary project that consisted of three sub-projects, each concerned with a similar kind of research -- the development of artificial adaptive systems with capabilities similar to those of their biological counterparts. Recent work on neural networks has demonstrated their potential for solving difficult problems in simplified, controlled environments. The next stage in the development of neural networks is their extension to the scale, complexity, and variability of real-world situations. This will not be a simple evolution of existing neural net designs, because it requires the integration of complex adaptive systems whose components have widely differing functions. Fortunately, biological organisms present existing solutions to this problem and neuroscience can now probe in detail the relevant structures. Biological systems are highly adaptive and operate well in extremely complex and variable environments. They accomplish this by partitioning the system into functional subunits in a quasi-hierarchical structure of neural network modules. In this project we have studied a number of specific examples of this system integration strategy and have modeled their operation for the purpose of creating new neural network architectures and control schemes.

The three sub-projects, which are fully described in Sections I, II, and III of this report, are introduced below:

I. Self-Supervised Learning Within a System of Map-Like Neural Networks

Many of the nuclei of the central nervous system exhibit map-like architectures, in which neuronal response characteristics exhibit a systematic spatial variation over the nucleus. These systems are examples of how to break large, complex problems down into smaller, simpler subproblems, and an understanding of them may provide insight into the construction of similarly powerful solutions in the technological domain. The target localization system in the barn owl is a particularly good example. The results include biophysically realistic models and computer simulations of the auditory localization system of the barn owl. We have produced many experimental predictions and greatly increased our understanding of how this system computes.

II. Modeling Adaptive Processing in the Visual Cortex

This project investigated the adaptive processing of motion signals by the visual cortex. In general, this system can be described as a chain of adaptive sub-modules, each of which adjusts the gain of selective components of its input signal. The result is a signal for which *change* in various relevant stimulus dimensions is emphasized. The results include a model of differential motion sensitivity in the cortex. Such results are useful not only for gaining insight into neural function, but also for improving the sensitivity of artificial vision systems to specified signal dimensions.

III. Hierarchical Architectures and Integration of Neural Networks and Knowledge-Based Systems for Intelligent Robotic Control

The objective of this research was to study the feasibility of using robotic skill acquisition for the intelligent control of highly redundant, anthropomorphic robotic manipulators. The control scheme uses models of human motor skill acquisition to guide the integration of knowledge-based systems and neural networks, and parallels the training of an athlete by a coach whereby the robot learns through experience how to perfect tasks initially specified in a high level task language. Knowledge-based system components are used to encode neural network learning strategies, and skill acquisition is associated with the shift from a predominantly feedback-oriented, knowledge-based representation of control to a predominantly feedforward, network-based form. Intelligent robotic control systems have been constructed with a hierarchical and modular organization, using antagonistic actuation mechanisms and multi-joint motor synergies.

Section I

Self-Supervised Learning Within a System of Map-Like Neural Networks

A. BACKGROUND

Most of the visual, auditory, and somatosensory nuclei of the central nervous system exhibit map-like architectures, in which neuronal response characteristics exhibit a systematic spatial variation over the nucleus. These map-like nuclei appear to serve as modules within hierarchical and parallel computing systems. These systems are examples of how to break large, complex problems down into smaller, simpler sub-problems, and an understanding of them may provide insight into the construction of similarly powerful solutions in the technological domain. In addition, they exhibit other useful properties for man-made computing systems, such as self-organization, self-optimization, and fault-tolerance. The neural substrate for target localization in the barn owl is one such system.

The barn owl can hunt in total darkness, recognizing and locating prey by hearing alone. One component of this behavior is a very accurate head-orienting response to salient sounds (the head must rotate as the eyes are immobile). This head saccade centers the sound-producing object for closer visual and acoustic scrutiny, prior to aerial attack. In the laboratory, owls can be trained to produce naturalistic head saccades to controlled sounds, and thus indicate the perceived sound location. In this way, the barn owl has been shown to be more accurate at localizing sounds than any other terrestrial animal studied thus far [12].

Considerable progress has been made in determining the acoustic and neural bases of the head saccade (see Fig. 1). The following description is greatly simplified, as its purpose is limited to providing the context for the work reported here (see [15, 7] for recent reviews). The acoustical properties of the owl's head and ears lead to the encoding of stimulus azimuth and elevation by interaural time delay (ITD) and interaural level difference (ILD), respectively [18]. In effect, associated with each direction in space there is a unique relationship between frequency (F), ITD, and ILD; to determine the direction of a sound source, the system must, in effect, compute the nonlinear mapping between the ITD and ILD spectrum of the sound and its direction.

The binaural ITD and ILD information is extracted in two steps. First the monaural timing and intensity information are separated by the cochlear nuclei [26]. Second, maps representing the ITD [27] and ILD [16] spectra are produced in, respectively, nucleus laminaris (NL) and the nucleus ventralis lemnisci lateralis pars posterior (VLVp).

Our previous modeling suggested that the merger of ITD and ILD should occur in two stages, in order to avoid the problem of phantom targets in multi-sound environments [22]. In the first stage, presumably the lateral shell of the central nucleus of the inferior colliculus (ICL), cells are tuned to unique combinations of ITD, ILD, and frequency, and arranged in a three-dimensional map. In the second stage, each of the ICL neurons projects to and excites the region of the space map in the ICX that corresponds to the direction associated with the ITD/ILD/F triplet to which it is tuned. Experimental work is in basic agreement with this model [4], but many details remain to be worked out. In any case, the equivalent of an "acoustic retina" is found in the external nucleus of the inferior colliculus (ICX) [13, 14].

In the optic tectum, projections from the ICX [10] and the retina produce a fused visual-acoustic representation of target direction [11], and both sensory maps are in register with a motor map of head saccade vector [3]. The visual/auditory alignment must be dynamically adjusted while the head is growing, because the changing shape of the head alters the relationship between ITD, ILD, frequency, and sound direction. The tectal auditory map shifts so as to stay in alignment with the tectal visual map [6, 8, 9]. This could easily be explained by correlation-driven

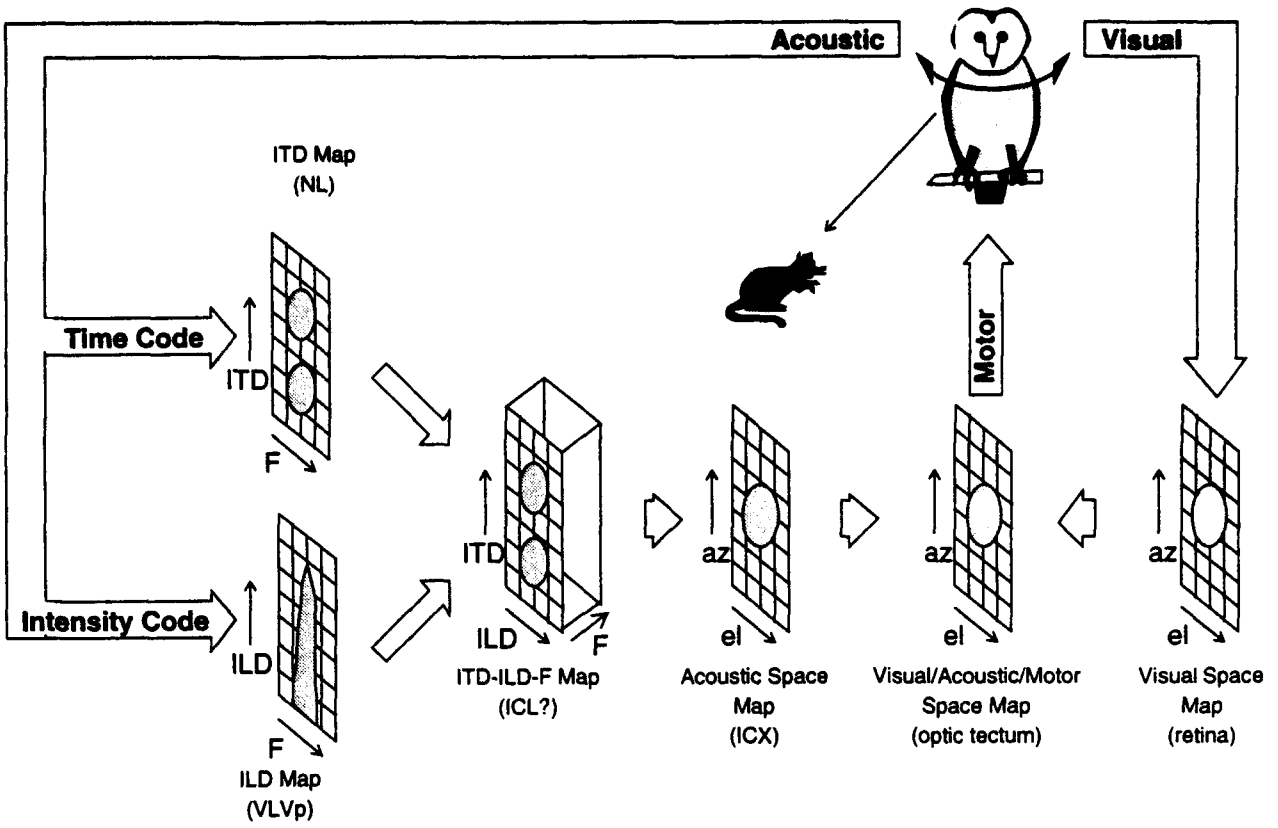

Figure I-1. Overview of the neural system for auditory localization in the barn owl. The grids indicate the map-like representation of information at each processing stage or nucleus. The "blobs" indicate the pattern of neuronal activation on the map in response to a typical stimulus. Acronyms NL, VLVp, ICL, ICX, ITD, and ILD are defined in the text. Arrows indicate the direction of signal flow. Symbols "az" and "el" denote azimuth and elevation, respectively, while F denotes frequency.

synaptic plasticity acting within a one-to-many ICX-to-tectum projection, and we in fact proposed such a model [19, 5]. However, shortly after this contract began, the Knudsen lab demonstrated that the plasticity is upstream of the tectum, in the inferior colliculus [1, 17]. This implies that the visual feedback must be indirect, as there are no known visual sensory inputs to the inferior colliculus.

B. OBJECTIVES

The purpose of this project was to further the understanding of this system through the development of biophysical and computational models and computer simulations. The goal was to produce explicit, testable predictions for neuroscience. In addition, it was expected that this research would lead to new artificial neural network designs, with applications for signal processing, sensory fusion, and sensorimotor integration.

C. RESULTS

1. Modeling the Intensity System

Instead of modeling the ICL-to-ICX projection and visual/auditory plasticity, as originally proposed, we chose to model the intensity processing system in the VLVp and ICL. This change

was made for several reasons in response to experimental reports made after the proposal was written. Fujita [4] reported that the ICL contained both ILD-tuned and ILD-sensitive neurons, and that there was some convergence across frequency in the ICL. Our previous model of the ICL incorporated only ILD-tuned cells and had no frequency convergence. Also, as mentioned above, the Knudsen lab showed that the visual/auditory plasticity was occurring upstream of the tectum [1,17]. Therefore it was decided to first construct a model of the ICL that could account for these findings before using it to model the formation of the space map in the ICX and visual/auditory fusion. This of course requires models of the inputs to the ICL. The nature of the representation of ITD prior to the ICL was quite well understood, however the representation of intensity and ILD prior to the ICL was not. However, the publication of Carr's anatomical study of the VLVp [2], along with Manley's physiological paper [15], gave us enough information to attempt a model and simulation of the VLVp. Therefore, we decided to develop joint models of the intensity processing of the VLVp and the ICL. The anatomical and physiological data to be incorporated and explained by our models of the VLVp and ICL are summarized in Fig. I-2, below.

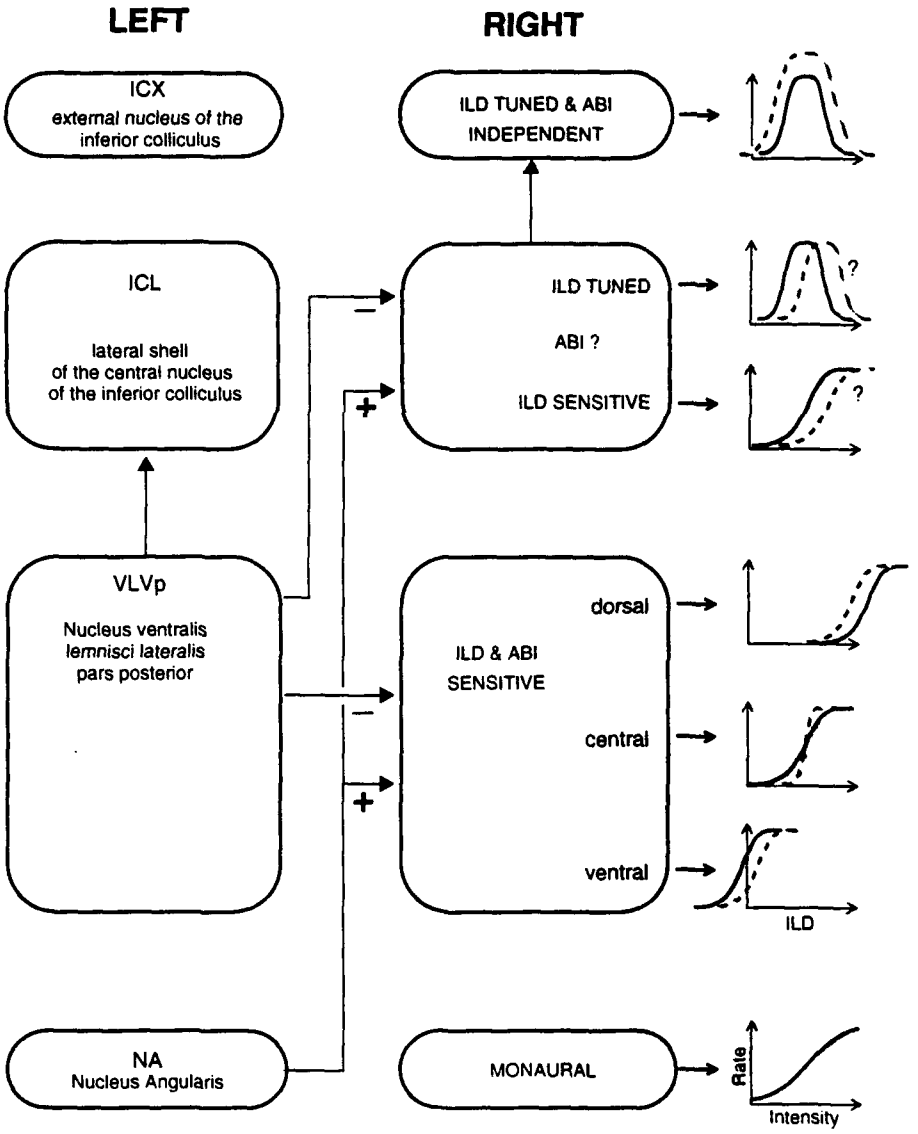

Figure I-2. The intensity processing system for sound elevation of the owl. On the left, the names and acronyms of the nuclei are given. On the right, the salient response characteristics are named and illustrated with graphs of stimulus response. The dashed curves represent the response with an increased average binaral intensity level (ABI). The "?" indicates that the ABI dependence is not completely known. The connections between nuclei are indicated by lines with arrows and the inhibitory and excitatory nature is indicated by "-" and "+", respectively.

The quantitative, mathematical network models developed were motivated by a qualitative model of the generation of ILD-selectivity, called the "spatial-derivative model". This model, illustrated in Fig. I-3 (below), was developed independently by a number of investigators, including S. Volman, T. Takahashi, R. Adolphs, and the personnel of this contract. The spatial-derivative model holds that a tone of a given frequency produces a wedge-like pattern of activation in the VLVp, and that for a fixed ABI, the position of the edge varies roughly linearly with ILD. Such a pattern of activation is suggested by the observed dorso-ventral variation of ILD-threshold depicted in the graphs of Fig. I-2. The model predicts that a peak-like pattern of activation is created along the medio-lateral axis of the ICL, from the wedge-like pattern in the VLVp. The location of the peak of activation would vary roughly linearly with ILD, which is clearly consistent with ILD-tuned responses.

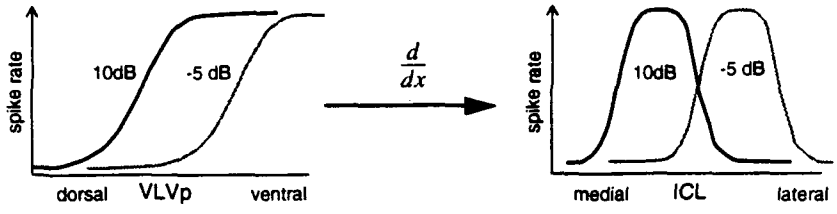

Figure I-3. The spatial-derivative model of ILD-selectivity in the ICL. The curves illustrate the hypothetical activation patterns within the VLVp and ICL for stimuli with ILD's of 10dB (solid) and -5dB (grey).

The first version of the network model of VLVp/ICL was presented in December, 1989 at NIPS [23], and at the Annual Meeting of the Society for Neuroscience. The anatomy of this model is summarized in Fig. I-4, below.

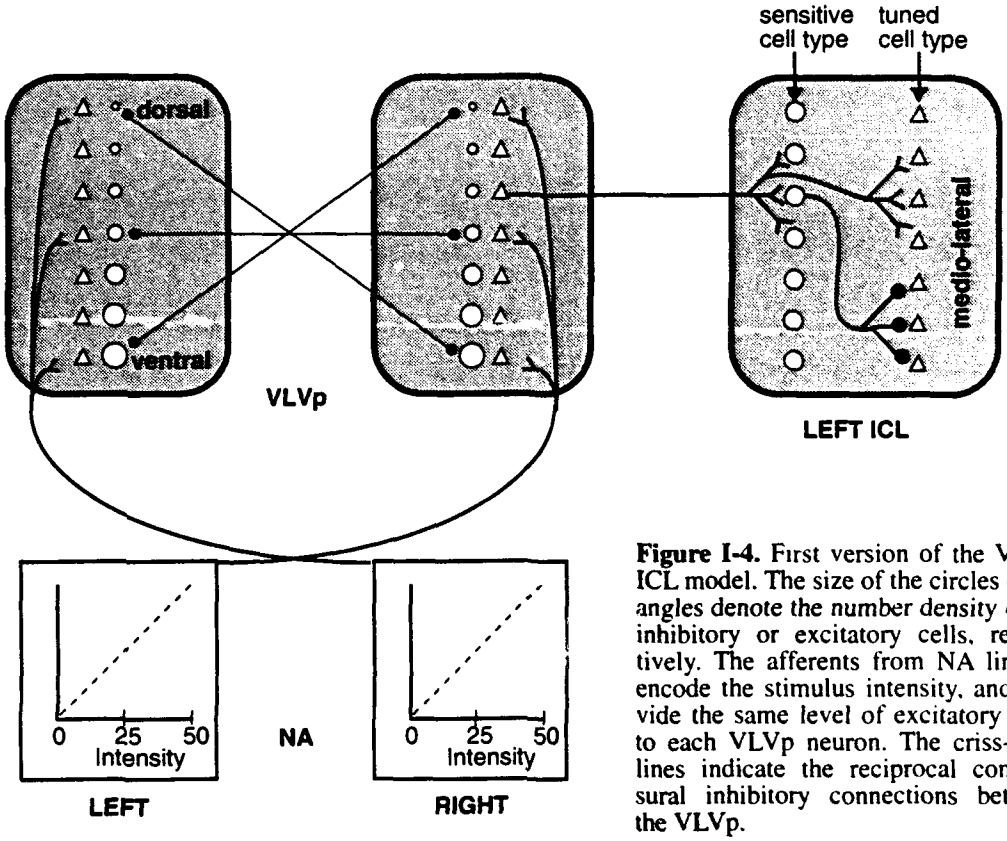

Figure I-4. First version of the VLVp/ICL model. The size of the circles or triangles denote the number density of the inhibitory or excitatory cells, respectively. The afferents from NA linearly encode the stimulus intensity, and provide the same level of excitatory drive to each VLVp neuron. The criss-cross lines indicate the reciprocal commissural inhibitory connections between the VLVp.

All VLVp neurons receive the same level of excitatory drive from NA. There is a criss-cross pattern of commissural inhibitory connections, which are reciprocal. Cells at one dorsal-ventral position inhibit the cells at the corresponding position of the contralateral VLVp, and vice versa. The reciprocity is not symmetric, as the ventral-->dorsal connection is stronger than the dorsal-ventral connection because of the gradient of inhibitory cell density. The reciprocally connected cells thus compete–whichever cells initially receive more excitation than inhibition will drive the output of their contralateral competitor towards zero while their own output rises towards the maximal level. Simulations showed that a wedge-like pattern of activation is produced (see Fig. I-5), in which the dorsal-ventral position of the "edge" of activation is linearly related to the stimulus ILD (see Fig. I-10), consistent with the spatial derivative model. This model was called the

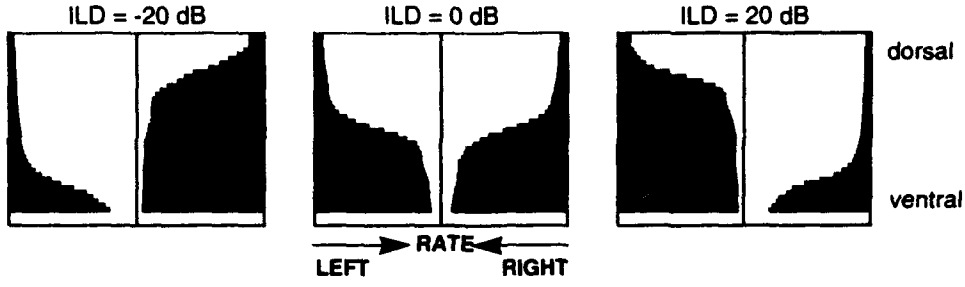

Figure I-5. Wedge-like dorsal/ventral activation patterns in the VLVp.

"competitive edge model" of the VLVp. The model also mimicked the VLVp stimulus response data of Manley, Koppl and Konishi [16], and the ICL stimulus response data of Fujita [4].

Early in 1990 a refinement of the VLVp model was made. A second population of local inhibitory neurons was added, which received the same inputs as the commissurally projecting neurons, but had the opposite density gradient, being more numerous at the dorsal surface, and less numerous at the ventral surface. These neurons acted to buffer the competitive dynamics, reducing the time it took the edge to form and reach its final position. This refined model was presented at the first meeting of the AMNS Workshop (July, 1990) [24], which included an in-depth review of the computational methods.

The ICL model was also modified during 1990, in light of recent unpublished data gleaned from discussions with experimentalists following our 1989 Society of Neuroscience presentation. The main factor was that the output from the VLVp to the ICL was inhibitory, and not excitatory as we had assumed in the first version of the model. This change could be made while staying within the framework of the spatial derivative model (described above). The architecture of this second model is illustrated in Fig. I-6, below. In revising the ICL model, we were greatly aided by discussions with Ralph Adolphs of CalTech, a graduate student in the Konish Lab. Ralph was then performing studies of the effects of injecting various neural activity modulators in the VLVp. The second version of the VLVp/ICL model was first presented at the 1990 Annual Meeting of the Society for Neuroscience, and it included simulations which mimicked Ralph's neuromodulator experiments. This work was also presented at the 2nd AMNS workshop in the summer of 1991 [28].

One of the benefits of our modeling approach was that we could easily explore the temporal or dynamic consequences of model parameters. All model parameters had real physical units, and we could unambiguously relate the difference equation temporal change unit to a specific unit of physiological time. For example, we could measure how long it took for the dynamic competition in the VLVp to reach an equilibrium, in terms of milliseconds. This is what led us to introduce the local inhibitory cells in the VLVp (described above). Fig. I-7 shows the pattern of activation in the model for the first ten milliseconds following stimulus onset. Such a sequence could be displayed in very rapid sequence on the SUN workstations we used–100 milliseconds of network time could be simulated and concurrently viewed in a few seconds. This enabled ideas to be tried out and parameters tuned very quickly.

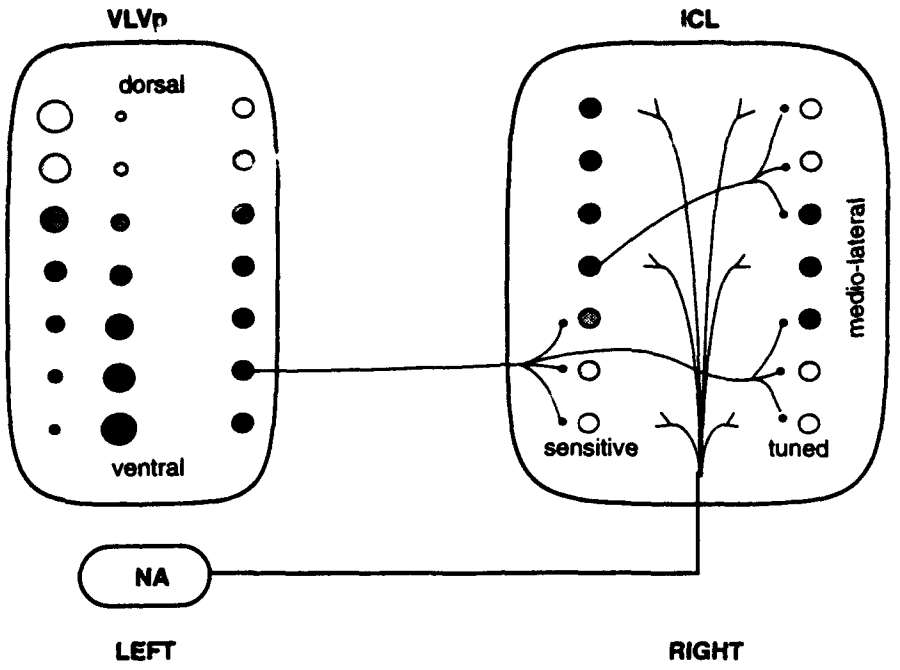

Figure I-6. Second version of the VLVp/ICL model. The stippling within the cells indicates the degree of stimulus-driven activation (the darker the more active).

Within the last year Ralph published detailed anatomical tracing studies [30] that suggest that the inter-VLVp inhibition is feedforward, rather than feedback, as it was assumed to be in our first (competitive-edge) model [28]. This finding contradicts earlier work by Takahashi [33],

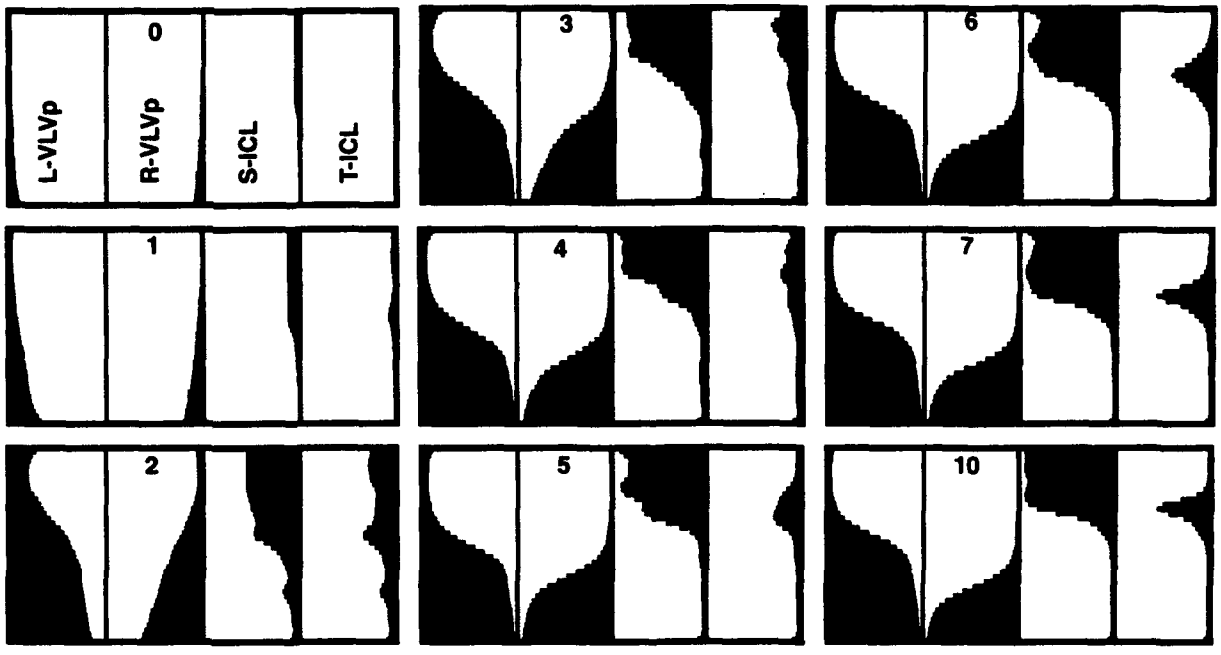

Figure I-7. VLVp/ICL activation pattern sequence. Each of the nine panels depicts the pattern of activation along the left and right VLVp, and the sensitive and tuned cells in the ICL, as indicated in the upper-left-hand panel. The numeric label (0, 1, 2, 10) is the number of milliseconds following onset. The patterns had stabilized by 10 milliseconds.

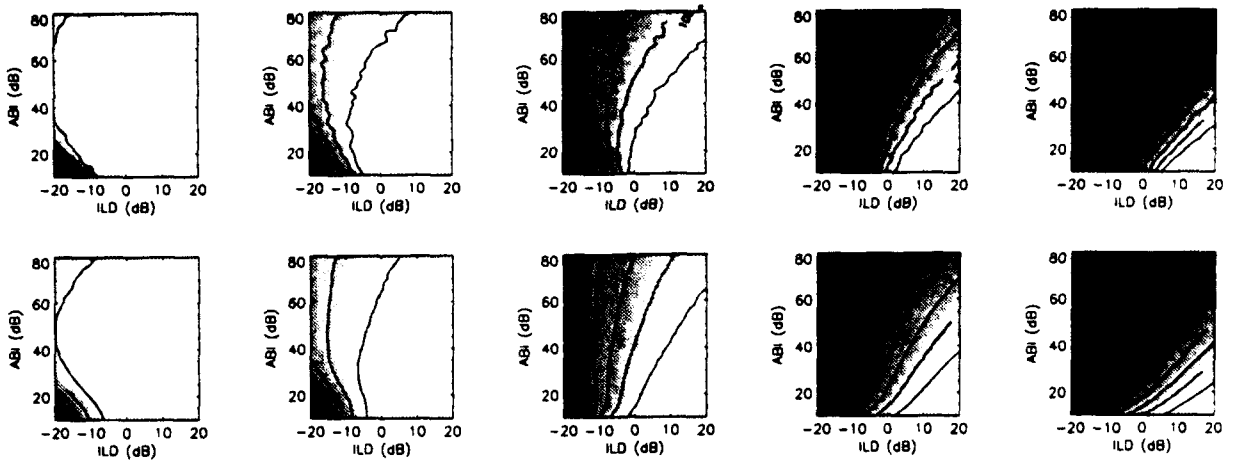

Figure I-8. Comparison of competitive-edge (top) and feedforward (bottom) models of the VLVp. The firing rate as a function of ILD and ABI is plotted. The 5 plots shown are taken from neurons spanning the dorsal-ventral dimension of the nucleus (depths of 25%, 37.5%, 50%, 62.5% and 75%), as can be surmised from the progressively shifting ILD thresholds.

whose HRP tracings were consistent with the competitive-edge model. In any case, we decided to explore whether a feedforward model could match the data of Manley et al. [16] as well as the competitive-edge model did. Our approach to this question was to train a static feedforward neural network to match the steady-state output of the competitive-edge model, using the techniques developed in the field of artificial neural networks. Work just completed demonstrates that the feedforward model can be trained so that the response curves are very similar to those of the competitive-edge model, as shown in Fig. I-8. The competitive-edge model is a closer match to the known anatomy in several other ways, and in our opinion, is still the best candidate. More anatomical experiments will have to be done to distinguish between these models. This is somewhat surprising, since the dynamics of the two models are so intrinsically different. This work was presented at the Society for Neuroscience Annual Meeting this year [32] and a manuscript is in preparation for submission to the Journal of Neuroscience.

Adolph's [30] also presented evidence that the VLVp--> ICL projection is bilateral, with the ipsilateral projection weaker than the contralateral projection. Previous work by Takahashi (unpublished, personal communication, Summer 1988) had revealed a contralateral-only projection, and this finding was an assumption of our previous ICL model. Conceptually, the presence of a bilateral projection does not invalidate our previous model, and in fact, bilateral projections could be incorporated in such a way that the resulting ICL responses and the underlying computational model ("spatial derivative model") would be the same. However, a bilateral projection does provide more degrees of freedom, and we were interested if perhaps an entirely different computational scheme could be implemented using it.

We were especially interested in deriving a new model of the VLVp --> ICL projection for which the dependence on the average binaural intensity (ABI) would be less in the ICL than in the VLVp. Our previous ICL model [28] was just as dependent on ABI as the VLVp. This is because the underlying spatial derivative model is based on point-to-point, topographic projections, and so the ICL must inherit the same degree of ABI dependence as the VLVp. The degree to which neurons in the ICL, ICX, and optic tectum are independent of ABI has not been extensively studied. It has generally been maintained that ICX and tectal cells are relatively independent of ABI [7]. This is what one would expect, since these neurons are thought to encode sound source direction, which is independent of ABI. However, there is also evidence from Olsen et al. [31] that tectal cells show the same kind of dependence on ABI that VLVp cells do [16].

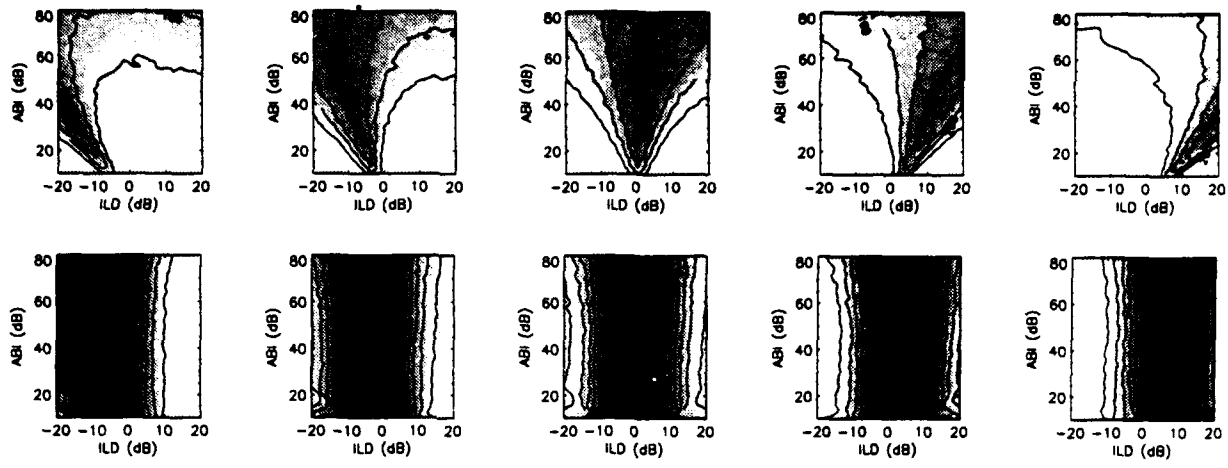

Figure I-9. Comparison of the "spatial-derivative" (top) and the "ABI-independent trained" (bottom) models of the ICL. The firing rate as a function of ILD and ABI is plotted for the tuned cells. The 5 plots shown are taken from neurons spanning the medio-lateral dimension of the nucleus (relative distances from one border of 25%, 37.5%, 50%, 62.5% and 75%), as can be surmised from the progressively shifting ILD peaks. Note the striking difference in the ABI dependence.

Our approach was to use the training methods of artificial neural networks to derive the connections between the VLVp and the ICL, as well as those within the ICL. We found that nearly ABI independent cells can be produced in the ICL, as illustrated in Fig. I-9. However, the ipsilateral projection from the VLVp was not essential for this. Models with the full bilateral projection were slightly more ABI independent than those with a contralateral-only projection, but the difference was not large.

As expected, analysis of the resulting trained network revealed that it is based on a different computational scheme than the spatial-derivative model. Rather than being point-to-point, the projection onto an ICL neuron comes from a wide region of the VLVp, as illustrated in Fig. I-10. At large ILD the cell fires at its highest rate. The excitatory input from NA is at a maximum and the inhibition from VLVp is at a minimum, since the active VLVp cells are to the right of the connection peak. As ILD decreases so does the cells firing rate. The VLVp inhibition increases as the wedge of activation extends into the range of the connection peak, and the excitation from NA decreases. ABI independence is achieved through a balancing act between excitation and inhibition. For a given ILD, as ABI increases, the activation pattern in the VLVp shifts such that the inhibition to ICL increases. At the same time, the excitation from NA increases and nullifies the increased inhibition. This "ABI-independent trained" model shows one way in which ABI independence can be achieved. Experimental work is needed to measure the actual degree of ABI independence, and confirm the nature of the predicted connection patterns. This work was presented at the CNS Conference this summer, at the Society for Neuroscience Annual Meeting this year [32], and a manuscript is in preparation for submission to the Journal of Neuroscience.

2. Modeling Time Delay Hyperacuity in Nucleus Laminaris

The auditory system of the barn owl contains neurons sensitive to the phase of sounds of remarkably high frequency, up to 9 kHz. Nucleus Laminaris (NL) represents phase differences as part of the computation of stimulus azimuth [27]. The input to NL is from both of the monaural magnocellular nuclei (NM). NM neurons encode stimulus phase or time by firing action potentials preferentially near a particular phase of the stimulus [26]. However, there is significant jitter in the phase at which the action potentials occur, which is noise in the input to NL. Furthermore, NM neurons cannot fire during every period of the sound at such high frequencies, so the number of spikes arriving at a laminaris neuron from each side of the head varies considerably from one

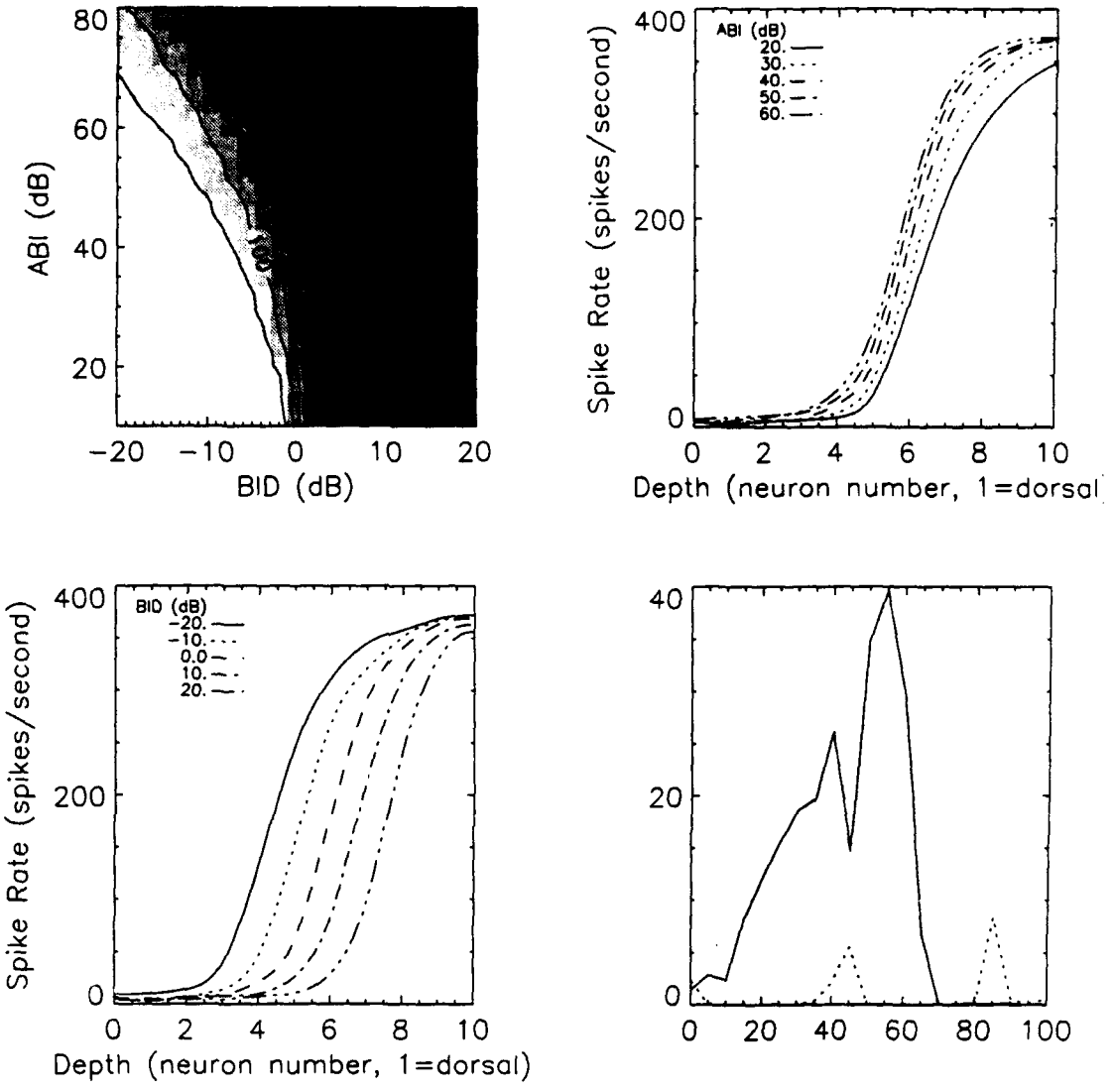

Figure I-10. Analysis of a sensitive cell in the "ABI-independent trained" model of the ICL. The upper-left panel is the ABI vs. ILD (or BID) response of the cell (compare with Fig. I-8 to see the reduction in ABI-dependence, this reduction was much more dramatic in other sensitive cells). The upper-right panel shows, for a given ILD, the nonlinear shift of the VLVp activation pattern as a function of ABI. The lower-left panel shows, for a given ABI, the linear shift of the same pattern as a function of ILD. The lower-right panel is the connection strength pattern from the VLVp onto the sensitive cell in the ICL. The solid and dashed lines are the contralateral and ipsilateral connections, respectively.

sound period to the next, giving an additional source of noise. The high frequency of the stimulus and the high level of noise in the input spike trains make the response properties of laminaris neurons hard to explain, and casts doubt on the common picture of NL neurons as coincidence detectors. We used simulations and semi-numerical analysis to show that the cellular and synaptic time constants must be very fast, probably unreasonably so, in order for ordinary biophysical mechanisms to reproduce the observed behavior.

Several people have suggested that a resonance mechanism may exist in laminaris neurons to amplify the signal. We investigated a simple neuronal resonance model that improved the performance considerably, but the synaptic and cellular time constants still had to be very fast, and we did not propose a specific biophysical resonance mechanism. This work was published in the proceedings of the second AMNS Workshop [29].

There is one peculiar feature of NL that may explain its ability to deal with high frequencies. In the presence of a sound, there is an extra-cellular potential in NL that oscillates in phase with the sound. This is called the neurophonic potential. Its exact amplitude has not been measured, but it may be in the range of 1 to 10mv [Ted Sullivan, personal communication]. The most likely sources of the neurophonic are the NM axons, which are carrying phase-locked spikes whose external fields would add coherently. This signal has relatively little noise simply because it is an average over thousands of the noisy signals from individual NM axons. We have calculated how a passive model of an NL neuron with the experimentally observed cell morphology would respond to such an oscillating external potential. In essence, the cell acts like an electrode. The membrane at the cell body conducts very well at frequencies above 5 kHz, and the myelinated axon's membrane does not. The oscillating potential near the soma propagates through the soma's membrane and down the axon. As a result, the oscillating part of the potential difference across the membrane is quite small at the soma, but grows in magnitude to a maximum of significant size at some distance down the axon. Voltage-dependent channels respond to the potential difference, so if they can respond at these frequencies they can respond to the oscillating potential difference. This would be a much cleaner signal than the synaptic input from NM.

This model has two appealing features: (1) The computation of potential difference has very few assumptions. The only unknowns are the magnitude of the external potential and the ability of the neuron to fire in response to the high-frequency potential difference. The first of these unknowns needs to be addressed experimentally, the second can be investigated through simulations. (2) The model provides an explanation for the unusual appearance of NL neurons in electron micrographs, especially the lack of a spike-initiating zone at the beginning of the axon. These observations were made by Catherine Carr, who suggested that spikes may be initiated at the first node in the axon, but there was no known reason for the neurons to have this structure.

3. Other Related Work

In addition to his role as consultant to the research effort at Sarnoff, Dr. Sullivan pursued a number of neurocomputational research topics related to the theme of this contract. The following is his report.

Past work by myself an others had shown that the processing of information about stimulus timing and intensity are physically separated, and that neurons in the brainstem regions responsible for these two functions are anatomically distinct. However, while we know a lot about the anatomy and physiology of neurons in both the time and intensity pathways, we have a poor understanding of the relationship between a neuron's anatomical structure and its physiological function. In my work on the auditory brainstem, I have found that questions of structure-function interrelationships are best approached in systems for which the physiological function of a particular neuron is fairly well understood. That is, it is easier to ask why a cell with a specific processing function has a particular anatomical structure than it is to ask what the function of a given cell with a known structure might be. I have used this approach to investigate the possible role of dendritic processes in neurons that compute horizontal sound localization by measurement of interaural time differences and to examine what advantages dendrites might provide to neurons specialized for processing information about stimulus intensity. In these studies and others designed to investigate physiological mechanisms of both time and intensity processing, I have come to realize more clearly that the physiological mechanisms available to optimize selectivity in the time domain are drastically different and often diametrically opposed to those that work best for intensity. My work is beginning to provide clear physiological explanations for the functional segregation that is observed in the auditory system and suggests that an understanding of cellular mechanisms can also help to explain higher levels of neuronal organization as well. The time and intensity segregation seen in the auditory system can also provide insights into the similar organization of other sensory systems since for any sense for which the stimulus is a form of energy (e.g., sound, light, touch), both the spatial pattern of energy distribution (i.e., intensity)

across the sensory receptors and the temporal pattern changes in this distribution must be neurally encoded

a. Dendritic function in nucleus laminaris

I have refined and extended a model for dendritic function in binaural time comparison. Earlier theoretical and empirical work has established that this computation involves a cellular process called coincidence detection in which a cell's spike output depends on its receiving at least two separate, temporally synchronized synaptic inputs. Neurons that perform this task at low frequencies have a pair of long dendrites, each dendrite being innervated by synaptic inputs derived from the ear opposite to those impinging on the other dendrite. The modeling results suggest that these bipolar dendrites enhance the cell's selectivity for simultaneous inputs impinging on both dendrites as compared to coincidences of two inputs arriving on the same side. This function requires electrical isolation between the synaptic inputs from the two ears and therefore cannot be done without dendrites. However, the mechanism exploits a fundamental property of neuronal synaptic transmission (voltage saturation) and is therefore a general candidate for dendritic functions involving sensitivity or selectivity for specific spatial or temporal combinations of synaptic input. Further analysis of the model's predictions using more realistic periodic synaptic inputs shows that aspects of dendritic morphology such as length, branching patterns, and number can be understood in the context of the basic mechanism I am proposing.

b. Comparison of binaral phase processing at high and low frequencies

Anatomical and physiological evidence indicates that the possible mechanisms of binaural ume comparison that I have described do not (and in fact cannot) operate in neurons that perform this task at high frequencies (>5000 cycles/sec) in the barn owl. These cells have no dendrites and also have a different axon morphology. A large portion of the work was devoted to understanding the physiological process that can enable timing information to be extracted from signals whose time course is much faster than what is normally considered for neuronal processes. My investigations show that both the temporal properties of synaptic input (transmitter release, post-synaptic change in electrical properties) and the mechanisms of spike output need to be examined and that with modest changes in both of these areas, the function of these cells can be explained. Most recently, I have been studying the relationship between the stochastic behavior of the action potentials in the input neurons and the patterns of synaptic conductance change seen by the coincidence detector cells. These ongoing studies are providing some interesting and insightful results that should help to confirm the functional/physiological dichotomy between temporal and level (intensity) processing mechanisms discussed above.

c. Cellular mechanisms of intensity processing in nucleus angularis

I have applied a similar logic to the one used to investigate time comparison mechanisms to an analysis of dendritic function in the processing of stimulus intensity. In this case, I have concluded that some of the intensity averaging functions that had been thought to be done by dendrites are not likely to be what dendrites are for since these functions can be done more efficiently in an adendritic cell. Rather, I am proposing a novel dendritic function for these cells: enhancement of the dynamic range of synaptic strength between threshold and saturation. This and other work that I have done suggests that the comparison of optimal morphological parameters obtained with different assumption about function is likely to provide a powerful approach to both the theoretical and empirical investigation of interactions between anatomy and physiology. I have begun a collaboration with Dr. Cathrine Carr at the University of Maryland designed to test some of the predictions of this work.

D. PUBLICATIONS

1. Pearson, J.C., C.D. Spence and R. Adolphs, "Model of the Origin of Neuronal Selectivity for Binaural Intensity Difference in the Barn Owl," Analysis and Modeling of Neural Systems II, F. Eeckman, ed, Kluwer, Boston (1993)
2. Spence, C.D. and J.C. Pearson, "A Resonance Model of High Frequency Binaural Phase Sensitivity in the Barn Owl Auditory Brainstem," Analysis and Modeling of Neural Systems II, San Francisco, July 1991.
3. Pearson, J. C., and C. D. Spence, "Model of the Computation of Auditory Stimulus Direction and Tuning to Interaural Level Difference in the Inferior Colliculus of the Barn Owl," *Society for Neuroscience Abstracts* **15** (50.6), 114 (1989).
4. Pearson, J. C., C. D. Spence, and R. Adolphs, "The Computation of Sound Elevation in the Barn Owl: Model and Physiology," *Society for Neuroscience Abstracts* **16** (299.3), 718 (1990).
5. Spence, C. D., and J. C. Pearson, "The Computation of Sound Source Elevation in the Barn Owl," *Advances in Neural Information Processing Systems 2*, edited by D. S. Touretzky (Morgan Kaufmann, San Mateo, CA, 1990), pp. 10-17.
6. Spence, C. D., and J. C. Pearson, "Models of the Computation of Sound Elevation in the Barn Owl," *Proceedings of the Analysis and Modeling of Neural Systems Workshop*, Berkeley, CA (1992).
7. Sullivan, W. E., "Resolution of μsec Timing in a Neural Compartmental Model," *Society for Neuroscience Abstracts*, **16** (360.3), 871 (1990).]
8. Sullivan, W.E., "Temporal Hyperacuity and Single Neuron Selectivity: Microsecond Time Resolution in a Neural Compartmental Model," *J. Comp. Physiol.* (Being Revised)
9. Sullivan, W.E., "Modeling High-Frequency Interaural Phase Comparison in Nucleus Laminaris of the Barn Owl," *Journal of Neuroscience* (Submitted).
10. Sullivan, W.E., "Mechanisms of Low Frequency Binaural Phase Comparison: Possible Function of Bipolar Dendrites," *Journal of Neurophysiology* (Submitted).
11. Sullivan, W.E., "Horizontal Sound Localization at High and Low Frequencies: The Biophysics of Structure-Function Correlations in Nucleus Laminaris," *Computational Neural Systems 1992 Symposium book*, (1992) (In press).
12. Sullivan, W.E., "Possible Mechanisms of High Frequency Phase Comparison in Barn Owls," *Society Neuroscience Abstracts* **17**: 446. (1991)
13. Pearson, J. C., and C. D. Spence, "Back-Propagation Generation of Hypotheses for the Projection Patterns which Give Rise to Neurons Tuned to Interaural Level Differences in the Barn Owl's Midbrain," *Society for Neuroscience Abstracts*, Volume **19**, pp. 530 (1993)

E. REFERENCES

1. Brainard, M. S. and E. I. Knudsen, "The Inferior Colliculus is a Site of Plasticity in the Visual Calibration of Auditory Spatial Tuning in Developing Barn Owls," *Society for Neuroscience Abstracts* **16**, 828 (1990).
2. Carr, C. E., I. Fujita, and M. Konishi, "Distribution of GABAergic Neurons and Terminals in the Auditory System of the Barn Owl," *The Journal of Comparative Neurology* **286**, 190-207 (1989).
3. du Lac, S. and E. I. Knudsen, "Neural Maps of Head Movement Vector and Speed in the Optic Tectum of the Barn Owl," *Journal of Neurophysiology*, **63**, 131-146 (1990).
4. Fujita, I., and M. Konishi, "Transition from Single to Multiple Frequency Channels in the Processing of Binaural Disparity Cues in the Owl's Midbrain," *Society for Neuroscience Abstracts* **15**, 114 (1989).

5. Gelfand, J. J., J. C. Pearson, C. D. Spence and W. E. Sullivan, "Multisensor Integration in Biological Systems," *Proceedings of the Third IEEE Symposium on Intelligent Control*, (1988).
6. Knudsen, E. I. and M. S. Brainard, "Vision Instructs the Auditory Spatial Tuning of Neurons in the Optic Tectum of Developing Barn Owls," *Society for Neuroscience Abstracts* **16**, 828 (1990).
7. Knudsen, E. I., S. du Lac and S. Esterly, "Computational Maps in the Brain," *Annual Review of Neuroscience*, **10**, 41-65 (1987).
8. Knudsen, E. I., "Experience Alters the Spatial Tuning of Auditory Units in the Optic Tectum During a Sensitive Period in the Barn Owl," *Journal of Neuroscience*, **5**, 3094-3109 (1985).
9. Knudsen, E.I. and P. F. Knudsen, "Vision Guides the Adjustment of Auditory Localization in Young Barn Owls," *Science*, **230**, 545-548 (1985).
10. Knudsen, E. I., and P. F. Knudsen, "Space-Mapped Auditory Projections from the Inferior Colliculus to the Optic Tectum in the Barn Owl (*Tyto alba*)," *Journal of Comparative Neurology*, **218**, 187-196 (1983).
11. Knudsen, E. I., "Auditory and Visual Maps of Space in the Optic Tectum of the Owl," *Journal of Neuroscience*, **2**, 1177-1194 (1982).
12. Knudsen, E. I., G. G. Blasdel, and M. Konishi, "Sound Localization by the Barn Owl (Tyto alba) Measured with the Search Coil Technique," *The Journal of Comparative Physiology*, **133**, 1-11 (1979).
13. Knudsen, E.I. and M. Konishi, "A Neural Map of Auditory Space in the Owl," *Science*, **200**, 795-797 (1978).
14. Knudsen, E.I. and M. Konishi, "Space and Frequency are Represented Separately in Auditory Midbrain of the Owl," *Journal of Neurophysiology*, **41**, 871-884 (1978).
15. Konishi, M., "Centrally Synthesized Maps of Sensory Space," *Trends in Neuroscience*, **9**, 163-168 (1986).
16. Manley, G. A., C. Koppl, and M. Konishi, "A Neural Map of Interaural Intensity Differences in the Brain Stem of the Barn Owl," *The Journal of Neuroscience*, **8**(8), 2665-2676 (1988).
17. Mogdans, J. and E. I. Knudsen, "Auditory Experience Modifies the Tuning for Sound Localization Cues of Neurons in the Barn Owl's Optic Tectum and Inferior Colliculus," *Society for Neuroscience Abstracts*, **16**, 828 (1990).
18. Moiseff, A., "Binaural Disparity Cues Available to the Barn Owl for Sound Localization," *Journal of Comparative Physiology*, **164**, 629-636 (1989).
19. Pearson, J. C., J. J. Gelfand, W. E. Sullivan, R. M. Peterson, and C. D. Spence, "Neural Network Approach to Sensory Fusion," C. B. Weaver, ed. SPIE, **931**, 103-108 (1988).
20. Pearson, J. C., and C. D. Spence, "Model of the Computation of Auditory Stimulus Direction and Tuning to Interaural Level Difference in the Inferior Colliculus of the Barn Owl," *Society for Neuroscience Abstracts*, **15** (50.6), 114 (1989).
21. Pearson, J. C., C. D. Spence, and R. Adolphs, "The Computation of Sound Elevation in the Barn Owl: Model and Physiology," *Society for Neuroscience Abstracts*, **16** (299.3), 718 (1990).
22. Spence, C. D., J. C. Pearson, J. J. Gelfand, R. M. Peterson, and W. E. Sullivan, "Neuronal Maps for Sensory Motor Control in the Barn Owl," *Advances in Neural Information Processing Systems 1*, edited by D. S. Touretzky (Morgan Kaufmann, San Mateo, CA, 1988), 366-374.
23. Spence, C. D., and J. C. Pearson, "The Computation of Sound Source Elevation in the Barn Owl," *Advances in Neural Information Processing Systems 2*, edited by D. S. Touretzky (Morgan Kaufmann, San Mateo, CA, 1990), 10-17.

24. Spence, C. D., and J. C. Pearson, "Models of the Computation of Sound Elevation in the Barn Owl," *Proceedings of the Analysis and Modeling of Neural Systems Workshop*, Berkeley, CA (in press).
25. Sullivan, W. E., "Resolution of μsec Timing in a Neural Compartmental Model," *Society for Neuroscience Abstracts*, **16** (360.3), 871 (1990).
26. Sullivan, W. E. and M. Konishi, "Segregation of Stimulus Phase and Intensity Coding in the Cochlear Nucleus of the Barn Owl," *Journal of Neuroscience*, **4**, 1787-1799 (1984).
27. Sullivan, W. E. and M. Konishi, "Neural Map of Interaural Phase Difference in the Owl's Brainstem," *Proceedings of the National Academy of Sciences USA*, **83**, 8400-8404 (1986).
28. Pearson, J.C., C.D. Spence, and R. Adolphs, "Model of the Origin of Neuronal Selectivity for Binaural Intensity Difference in the Barn Owl," Analysis and Modeling of Neural Systems II, F. Eeckman, ed., Kluwer, Boston (1993)
29. Spence, C.D. and J.C. Pearson, "A Resonance Model of High Frequency Binaural Phase Sensitivity in the Barn Owl Auditory Brainstem," Analysis and Modeling of Neural Systems II, San Francisco, July 1991.
30. Adolphs, R., "Bilateral Inhibition Generates Neuronal Responses Tuned to Interaural Level Differences in the Auditory Brainstem of the Barn Owl," *Journal Of Neurosciences*, **13**, 3647-3668 (1993).
31. Olsen, J. F., E. I. Knudsen, and S. D. Esterly, "Neural Maps of Interaural Time and Intensity Differences in the Optic Tectum of the Barn Owl," *Journal of Neurosciences*, **9**, 2591-2605 (1989).
32. Pearson, J. C., and C. D. Spence, "Back-Propagation Generation of Hypotheses For The Projection Patterns Which Give Rise to Neurons Tuned To Interaural Level Differences In The Barn Owl's Midbrain," *Society for Neuroscience Abstracts*, Volume **19**, pp. 530 (1993).
33. Takahashi, T. T. and C. H. Keller, "Commissural Connections Mediate Inhibition For The Computation of Interaural Level Difference In The Barn Owl," *Journal of Comparative Physiology A*, **170**: 161-169 (1992).

Section II

Modeling Adaptive Processing in the Visual Cortex

A. BACKGROUND

Hubel and Wiesel (1959, 1962, 1968), in exploring the visual cortex of the cat and monkey, found cells that responded selectively to motion of a bar or edge in a particular direction. Psychophysical evidence for similar direction-selective mechanisms in humans comes from Levinson and Sekuler (1975) and Watson, Thompson, Murphy, and Nachmias (1980). In these studies, contrast thresholds were measured for the detectability of a drifting sine grating, as a function of the contrast of a simultaneously present grating component (the mask) drifting in the opposite direction. The data showed that contrast thresholds were largely unaffected by sub-threshold mask contrasts, suggesting the existence in human vision of direction-selective mechanisms whose responses are independent of other concurrently responding mechanisms, at least at low stimulus contrast levels.

However, when stimulus contrasts rise above detection threshold, this independence among mechanisms appears to break down. Stromeyer, Kronauer, Madsen and Klein (1984) measured thresholds for changes in contrast of one or both components of a counterphase grating; i.e., the sum of two gratings of equal high contrast, and equal spatial and temporal frequencies, drifting in opposite directions at the same velocity. Their data showed much lower thresholds for changes involving the simultaneous increment and decrement of the two grating components, over changes involving increments of both components. This reduced effectiveness of the simultaneous increment is not predicted by a model in which the mechanisms sensitive to the two stimulus components are responding independently of each other. Instead, it suggests an inhibitory interaction in which each stimulus component is reducing the detectability of the other. This inhibitory interaction can be thought of as a gain-setting operation among the cortical mechanisms responding to a particular visual signal.

B. OBJECTIVES

The purpose of the work performed under this contract was to analyze quantitatively the form and possible utility of this cortical gain-setting operation. Using the signal domain of spatiotemporal variations in luminance, we undertook three tasks:

Task 1: Perform parametric psychophysical measurements of contrast discrimination among simple motion stimuli.

Task 2: Develop a cortical gain-control model that predicts the results of Task 1.

Task 3: Investigate signal-enhancing properties of the model developed in Task 2.

One result of Task 3, to be discussed below, is that the gain-control model exhibits a noise-cleaning function for quantum noise in spatio-temporal signals.

C. RESULTS

1. Task 1: Psychophysical measurements

In all experiments, contrast discrimination thresholds were measured among stimuli composed of the sum of a leftward and rightward drifting sine grating of equal spatial frequency and

equal but opposite drift rate. In all cases, the only adjustable stimulus parameters were the contrasts of the two grating components. Thus, all stimuli can be represented as points in a two-dimensional space of these two contrast settings, and the psychophysical task can be described in this same space (call it m2space) as follows: For a given point m2space (the mask point) and a given direction of excursion from that point (the test vector direction), find the magnitude of excursion for which observers reliably detect a difference between the stimulus at the mask point and the stimulus along the test vector. For measurements along a range of different test vector directions from the same mask point, the data can be represented as closed discrimination contours around the mask point, analogous to the Macadam ellipses of color discrimination measurements.

Fig.II-1 (below) shows some typical discrimination contour results. The solid line contours show the predictions of the model developed in Task 2, described below. The main point to observe here about these data is that the sets of threshold points (open circles with error bars) from each mask point (+ signs) tend to group themselves along rays from the origin of m2space. This grouping suggests a gain control process in which the outputs of mechanisms sensitive to opposite directions of motion inhibit each other with a division-like operation. Assuming that each mechanism responds linearly to the contrast of its input pattern, the grouping occurs because all points along a single ray have the same ratio of responses of the two mechanisms.

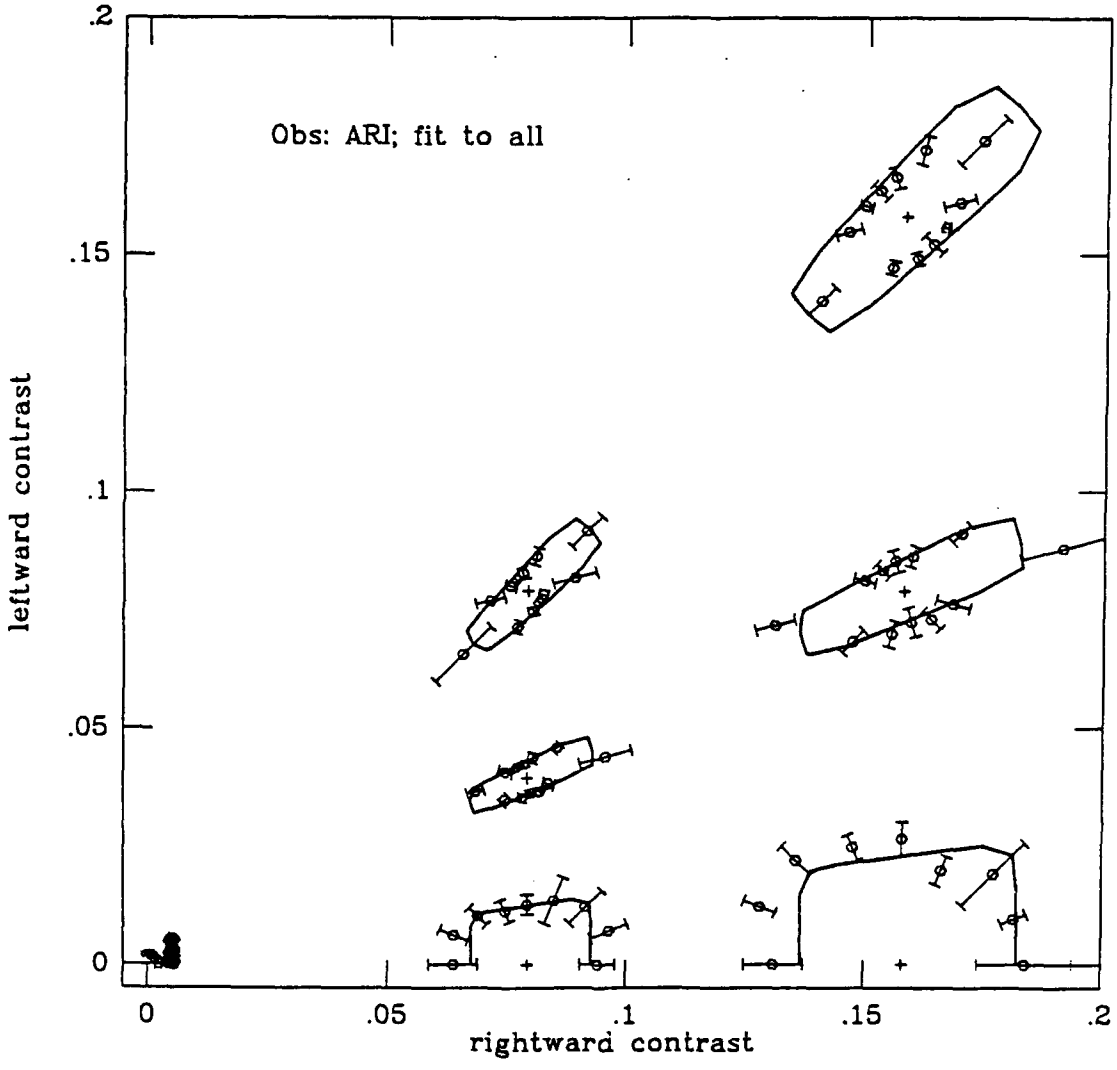

Figure II-1. Discrimination contours for observer ARI.

1. Task 2: Cortical gain control model

Fig. II-2 shows flow diagram for the cortical gain control model. The model consists of four main stages:

1. A **direction-selective mechanism** stage, at which the responses of simple mechanisms sensitive to leftward and rightward drifting gratings are calculated.
2. A **mechanism combination** stage, at which the outputs of the direction-selective mechanisms are combined to produce two opponent and one non-opponent mechanism outputs.
3. A **transduction** stage, at which each of the three outputs from the previous stage is passed through its own sigmoid non-linearity.
4. A **decision** stage, at which changes in the three outputs of the transduction stage from the mask to the test+mask stimulus presentations are used to choose which of the two stimuli contained the test.

At the core of the model is the opponent division operation indicated by the circular operators in the flow diagram. This opponent division turns out to have some interesting noise cleaning properties, as will be discussed in the next section.

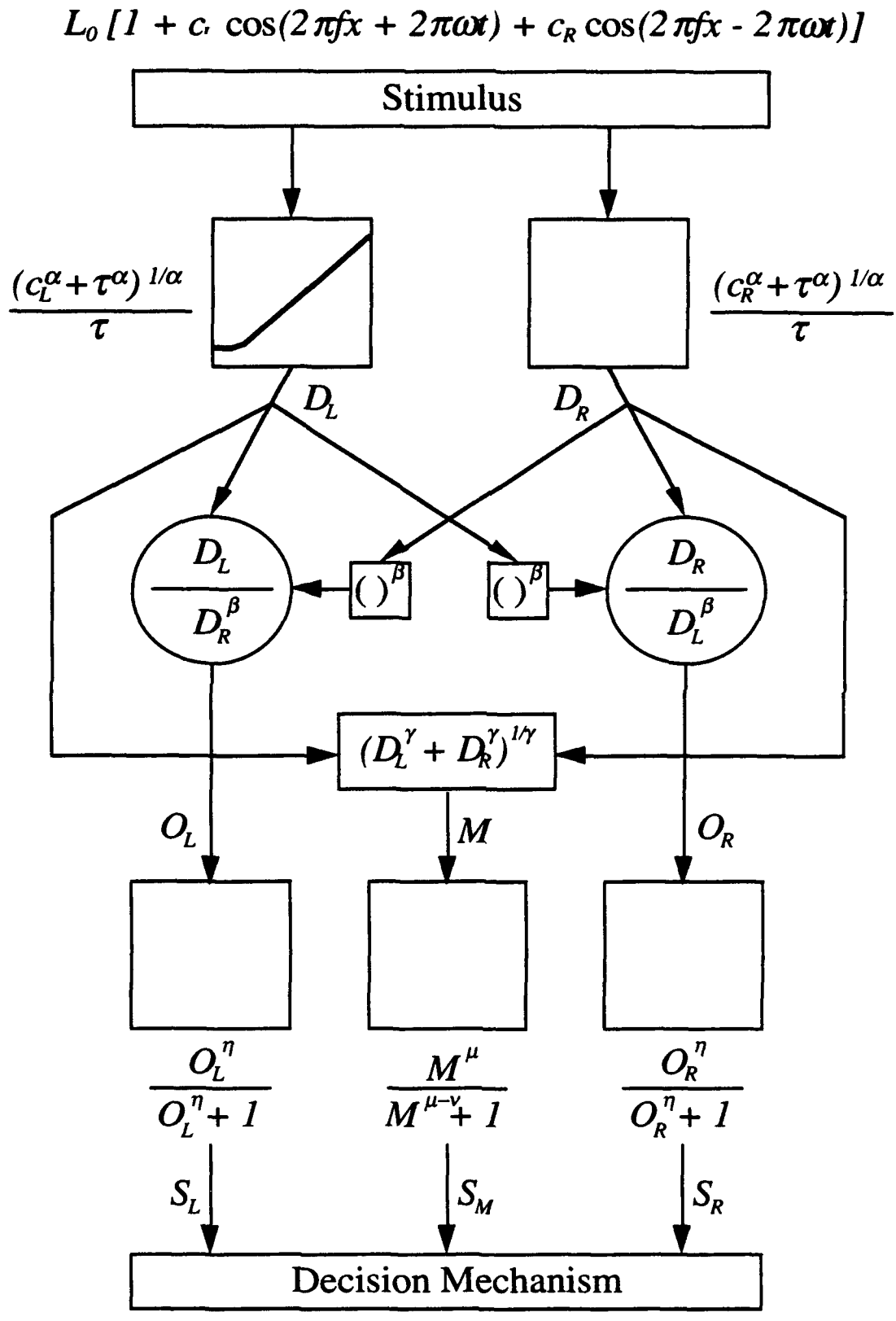

Figure II-2. Opponent vision model flow chart

2. Task 3: Signal enhancing properties

Fig. II-3 shows how the model developed to account for the psychophysical results described above can clean noise from spatio-temporal signals. Panel A of the figure shows two frames from a five-frame input sequence. These five frames were constructed from a field of filtered noise by displacing a central square by one pixel to the right on each frame, while the background move to the left by one pixel. Panel B shows the response of the model through the direction-selective mechanism stage. Note that the square region can now be seen, although it is partially obscured by noise. Panel C shows the response of the model after the opponent division operations. Notice that noise is now substantially reduced.

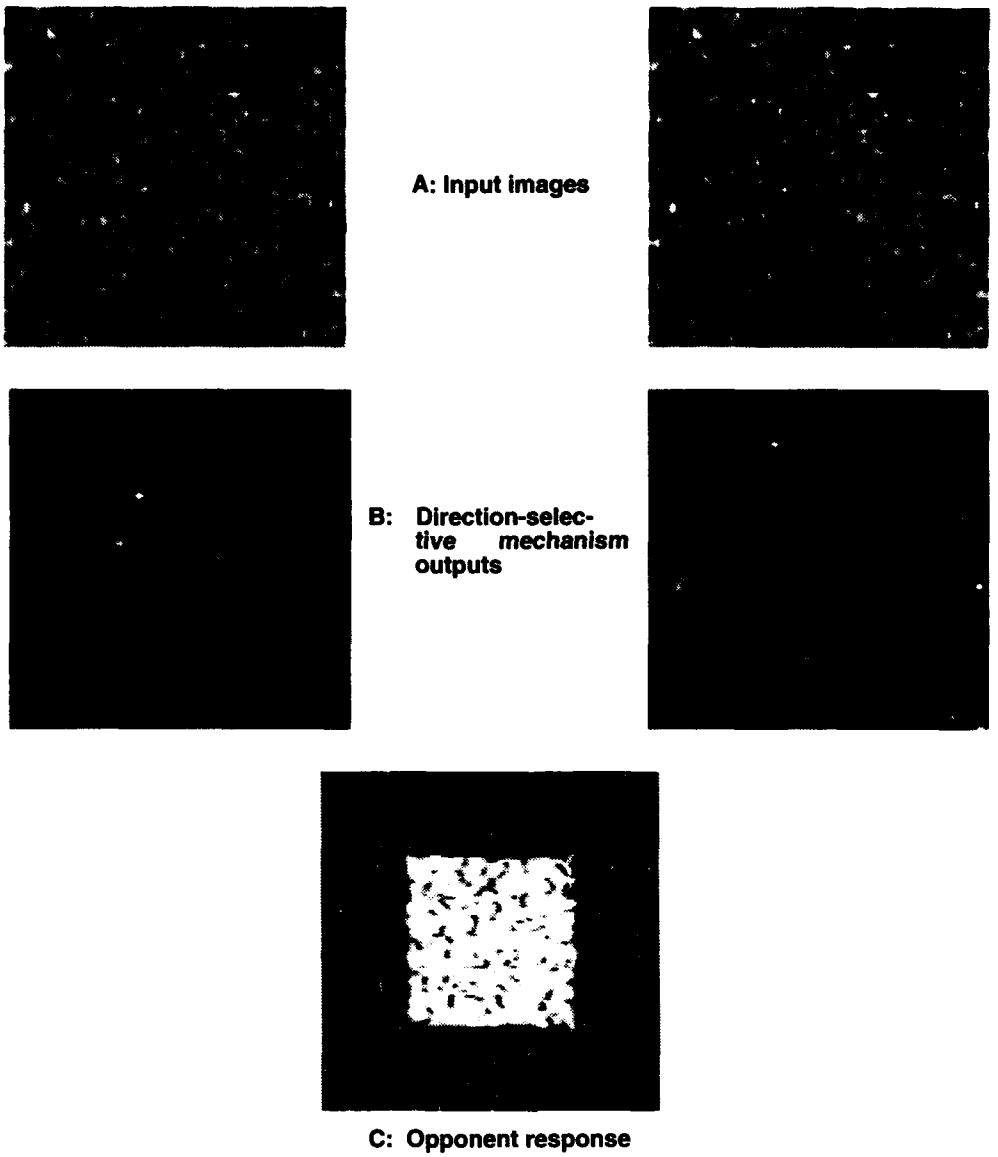

Figure II-3. Noise cleaning by opponent motion model.

This noise-cleaning feature of the opponent division model has been incorporated into a scheme for moving target indication, as is demonstrated in Fig. II-4. Here, video sequences taken

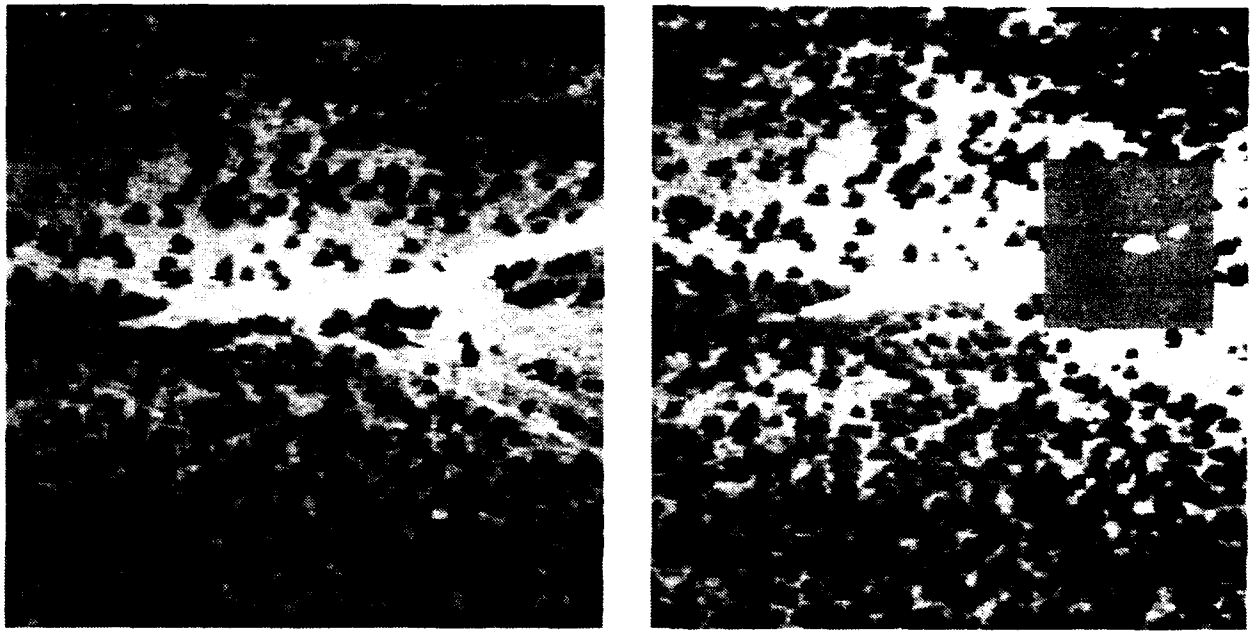

(a) (b)

Figure II-4. Moving target enchancement. (a) Original. (b) Enhanced with opponent motion operation.

from an in-flight helicopter scanning the ground have been enhanced to indicate the presence of vehicles moving along the ground.

The algorithm for this enchancement operation is as follows:

(1) Stabilize multiple frames from the image sequence to remove camera induced image motion.

(2) Within a region of interest on the resulting stabilized image sequence, compute motion energy for leftward and rightward motion (e_L and e_R). These energy computations are based on the outputs of Hilbert pairs of linear, spatiotemporally oriented filters.

(3) Then, at each point in the image plane, compute:

$$\frac{e_l - e_R}{e_L + e_R + k}$$

where k is a small additive constant that prevents division by zero, and also serves to remove small amounts of image noise. (The results are very insensitive to the exact choice of k, within a large range.)

Notice in Fig.II-4 that in each case the moving vehicle that is nearly invisible in the original sequence (Panel a) became, in the processed sequence (Panel b), an easily visible intensity peak that could be input to an automatic target tracking system, or used for visual reconnaissance.

D. PUBLICATIONS

1. Lubin, J., "Interactions among motion sensitive mechanisms in human vision," Ph.D. Dissertation, eupnea., 1992.
2. Lubin, J., "Adaptive coring techniques for spatio-temporal signals," *Proceedings of the IEEE Workshop on Visual Motion*, October 1991, pp. 333 to 339.
3. Lubin, J., "Pattern discrimination in the fovea and periphery," *Investigative Ophthalmology and Visual Science*, **32**, (4), p. 1024, May 1991.
4. Lubin, J., "Discrimination contours in an F/3F stimulus space," *Investigative Ophthalmology and Visual Science*, **31**, (4), p. 409, May 1990.

E. REFERENCES

1. Bonds, A. B., "Role of inhibition in the specification of orientation selectivity of cells in the cat striate cortex," *Visual Neuroscience*, **2**, 41-55, (1989).
2. Dean, A. F., R. F. Hess, and D. J. Tolhurst, "Divisive inhibition involved in direction selectivity," *Journal of Physiology (London)*, **308**, 84-85, (1980).
3. Lubin J., "Discrimination contours in an opponent motion stimulus space," *Investigative Ophthalmology and Visual Science Supplement*, **30**, 426, (1989).
4. Shapley R. and C. Enroth-Cugell, "Visual adaptation and retinal gain controls," *Progress in Retinal Research*, **3**, 263-346, (1984).
5. Poggio T. and V. Torre, "Ill-posed problems and regularization analysis in early vision," AI Lab Memo No. 773, MIT, Cambridge, MA, April (1984).
6. Hubel, D.H. and T. N. Wiesel, "Receptive fields of single neurons in the cat's striate cortex," *Journal of Physiology*, **148**, 574-591 (1959).
7. Hubel, D.H. and T. N. Wiesel, "Receptive fields, binocular interaction, and functional architecture in the cat's visual cortex," *Journal of Physiology*, **160**, 106-123 (1962).
8. Hubel, D.H. and T. N. Wiesel, "Receptive fields and functional architecture of monkey striate cortex," *Journal of Physiology*, **195**, 215-243 (1968).
9. Levinson, E. and R. Sekuler, "The independence of channels in human vision selective for direction of movement," *Journal of Physiology*, **250**, 347-366 (1975).
10. Watson, A.B., P. G. Thompson, B. J. Murphy, and J. Nachmias, "Summation and discrimination of gratings moving in opposite directions," *Vision Research*, **20**, 341-347 (1980).
11. Stromeyer, C.F. III, R. E. Kronauer, J. C. Madsen, and S. A. Klein, "Opponent-movement mechanisms in human vision," *Journal of the Optical Society of America A*, **1**, 876-884 (1984).

Section III

Hierarchical Architectures and Integration of Neural Networks and Knowledge-Based Systems for Intelligent Robotic Control

A. BACKGROUND

Most conventional robotic systems operate in structured environments and are quite unskilled by human standards, having trouble with such seemingly simple factory assembly tasks as picking a part from a bin or threading a nut on a bolt. One important ingredient lacking in these approaches is the system's ability to acquire sensorimotor skills through learning and practice.

One popular model of human skill acquisition [1] defines three phases of learning: (1) the cognitive phase, wherein a beginner tries to understand the task, (2) the associative phase, in which patterns of response emerge and gross errors are eliminated, and (3) the autonomous phase, when task execution requires little cognitive control. Knowledge can be represented in this skill acquisition model using declarative and reflexive forms of memory and learning [2]. Motions indicative of declarative memory and learning require conscious effort, are characterized by inference, comparison, and evaluation, and provide insight into not only how something is done, but why. Motions involving reflexive mechanisms relate specific responses to specific stimuli, are automatic, and require little or no thought.

Tasks initially learned declaratively often become reflexive through repetition. Conversely, when familiar tasks are attempted in novel situations, reflexive knowledge often must be converted back into declarative form in order to become useful. Furthermore, shifts from declarative to reflexive forms of control often are accompanied by a reduced dependence on sensory information [3,4], implying the utilization of learned predictive models of one's behavior and environment. This learning and shifting of task-specific knowledge between declarative and reflexive forms of memory plays a fundamental role in human skill acquisition, affecting computational resource allocation, the focusing of attention, and the ability to adapt.

In addition, humans typically rely upon visual information for motor control, but can with practice switch to proprioceptive control of motion [5-7]. This ability is particularly useful because vision is so effective for monitoring the environment and planning motion. For example, in sports, a novice must devote a great deal of visual attention to the control of his or her limbs and the execution of those tasks necessary for play. This restricts the visual resources available for monitoring the opponent or field position. On the other hand, an expert has learned, through practice, motor programs that rely for their execution predominantly upon kinesthetic input from limbs and muscles -- leaving vision free to attend to the other aspects of the game [8].

B. OBJECTIVES

The goal of this project was to develop intelligent sensorimotor control systems that integrate declarative and reflexive forms of processing and multisensory inputs within biologically inspired control hierarchies to enable high levels of robotic dexterity and adaptability. These approaches are to be tested on a high-degree-of-freedom robot. The following is a summary of the Statement of Work contained in the project proposal:

Task 1: Investigate models of the structural, functional, and behavioral aspects of human motor control and skill acquisition for the development of hierarchical processing architectures

for intelligent robotic control. Investigate how these biological paradigms might be used to integrate knowledge-based systems and neural networks for robotic skill acquisition.

Task 2: Develop advanced neural network modules for use in trajectory generation, reflex gain modulation, and inverse kinematic and dynamic transformations.

Task 3: Investigate how the resultant control technique might be applied to complex dynamic systems, including a high-degree-of-freedom robotic limb with low-level reflexes utilizing muscle-like pneumatic actuators. Investigate system performance associated with learning reflex gain modulations and set-point adjustments for functional motor control tasks.

C. RESULTS

1. Task 1

a. Intelligent control architecture

An architecture for intelligent sensorimotor control has been developed that emulates phases of human motor skill acquisition by integrating knowledge-based systems and neural networks. The robotic skill acquisition architecture depicted in Fig. III-1 (below), is modelled after the major structural and functional features of the human motor control system.

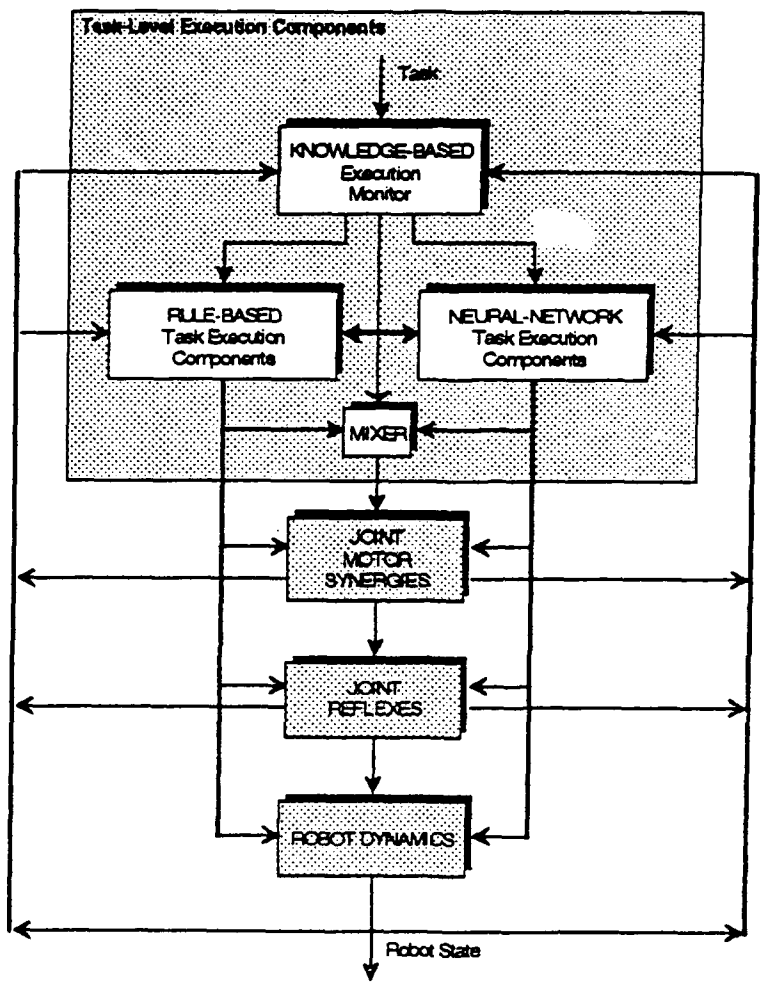

Figure III-1. Hybrid intelligent robotic control architecture

Three main levels of the control hierarchy are defined: joint reflexes, motor synergies, and task-level execution components. On the lowest level, each joint is endowed with reflexes (servo-mechanisms) that command torque as a function of sensed joint position, velocity and torque, and desired joint position, velocity, and acceleration. The reflexes are coordinated by motor synergies, the "spinal cord" of this architecture, so as to limit the number of degrees-of-freedom that actually need to be controlled by higher levels of the system. Task-level execution components invoke motor synergies most appropriate to the task at hand, then set the system in motion by providing the reflex loops and active motor synergies with time varying gains and commands needed to perform maneuvers. Motor synergy modulation and command generation are carried out by both rule-based and neural network-based task execution components, sometimes jointly, sometimes independently, with the execution monitor supervising various phases of learning through the manipulation of the mixer in Fig. III-1. The execution monitor continuously evaluates neural network task execution performance and re-engages rule-based components whenever errors due to changes in the dynamic system or its operating environment necessitate retraining of a network. The rule-based subsystems thereby ensure proper task completion while neural network re-learning takes place. The manner in which rules and networks interact during the various phases of learning and supervision gives this control architecture unique adaptive capabilities.

b. Robotic skill acquisition

In an attempt to capture behavioral features of human-to-human skill transfer, along with their implications regarding the management of attention and computation, our approach to robotic skill acquisition incorporates both declarative and reflexive forms of processing. This architecture utilizes transitions between declarative knowledge-based systems and reflexive neural networks to enable system adaptation and optimization. The control scheme attempts to parallel the training of an athlete (the robot) by a coach (the designer), whereby the robot learns through experience how to perfect tasks initially specified in a high-level task language. Rule-based system components encode neural network learning strategies, and skill acquisition is associated with the shift from a predominantly feedback-oriented, rule-based representation of control to a predominantly feedforward, network-based form.

In this case, the acquisition of skill is meant to imply a dramatic improvement in task performance over time, as well as a significant decrease in the amount of computation required to obtain this performance. A reduced computational burden is desired in order to mitigate the usually adverse effects of scaling up a problem, such as an explosive growth in the number of rules or execution time required to handle an increasingly complex control problem. Fig. III-2 depicts how

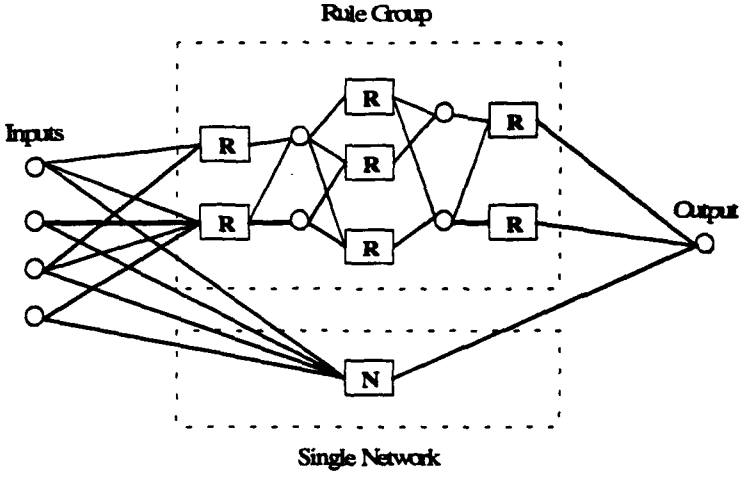

Figure III-2. Explicit and implicit functional dependencies provided by rules and neural networks within an RSA2 controller.

this reduction in computation, and hence execution time, is achieved here. Initially, explicit control strategies are conveniently represented by a hierarchical knowledge base. As the system operates, the input/output relationships encoded by inferencing rule-based resources are smoothly transformed into implicit neural network mappings.

Analogies to models of human motor skill acquisition are used to define transitions between declarative and reflexive modes of operation. The various phases of robotic skill acquisition are depicted in Fig. III-3. During the declarative phase, knowledge-based system components discover how to achieve rough-cut task performance. Rules and conventional control algorithms provide for plan specification, desired trajectory generation, and error-driven control commands. During the hybrid phase, neural networks learn by knowledge-based example how to accomplish parts of the task. Knowledge-based and neural-network-based components share control responsibility, with relatively poor initial network performance giving way to robust patterns of learned response. Finally, during the ***reflexive phase*** of skill acquisition, certain functions previously provided by inferencing rule-based resources are now provided by memory-intensive neural networks. If desired, associated rules are conditionally removed from the decision-making process. When applicable, reflexive neural network-based control is optimized through reinforcement learning.

Improvements in system performance during the transition from declarative to reflexive operation are accomplished using the neural network training paradigm of *feedback-error-learning*

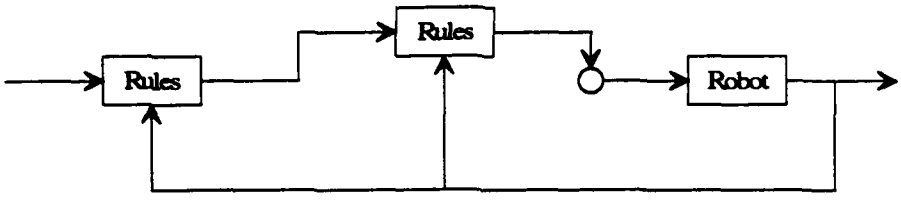

(a) Declarative Phase: plan specification, desired trajectory generation, and error-driven control commands provided by rule-based system components.

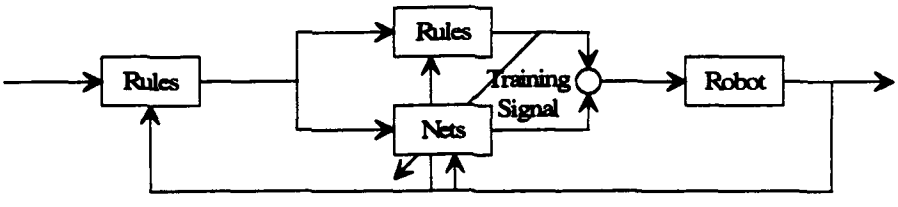

(b) Hybrid Phase: neural networks contribute to, and learn from, rule-based control commands.

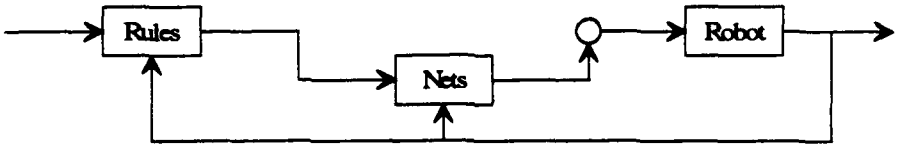

(c) Reflexive Phase: functions previously provided by inferencing rule-based resources now provided by memory-intensive neural networks.

Figure III-3. Shift in representation of control law during phases of robotic skill acquisition.

[9]. In feedback-error-learning, the total control command is the algebraic sum of two components: (1) an error-driven feedback component that ensures reasonable, yet improvable, system behavior, and (2) a neural network-based component that initially contributes nothing, but learns over time to compensate for the inadequacy of the feedback component:

Control Command = Feedback Component + Network Component (1)

In an RSA2 controller, the feedback component is knowledge-based, utilizing rules and conventional control algorithms to embed as much knowledge about successful control strategies as possible (or practical). During the Hybrid Phase of skill acquisition (Fig. III-3), the goal of neural network training is to minimize over time this feedback component's contribution to the control command, and thereby drive it to zero. Consequently, the feedback component's corrective actions, driven by discrepancies between desired and actual (measured or estimated) trajectories, not only serve as part of the control law, but also serve as neural network weight update errors. Given adequate feedback control suggestions and reasonable learning rates, the network component will learn the inverse dynamics of the system being controlled, in the sense that it can recall the control command required for a desired change in system output.

The learning philosophy embodied by feedback-error-learning, used here in conjunction with knowledge-based systems and neural networks, permits analogies to be drawn to certain aspects of human skill acquisition. A limited amount of strategic knowledge initiates motion. Performance improves incrementally through learning, with inferential problem solving giving way to reflexive motor programs. Computational efficiency is intended for areas of the dynamic state-space visited often, as in repetitive maneuvers. Inferential problem solving remains ready, however, to handle infrequently executed tasks, or changes in the robot or its environment that render previously acquired expertise ineffective. The RSA2 control technique provides a way to combine rules, neural networks, and feedback-error-learning to enable such adaptive behavior.

2. Task 2

a. Neural network architectures

The type of neural network architecture used in a control problem has a major impact on system learning and performance. It is well known that many biological sensorimotor control structures in the brain are organized using neurons that possess locally tuned overlapping receptive fields. The main benefits of using local approximation techniques to represent nonlinear system functions are faster learning, compared to the global approaches, and the ability to train the network in one part of the input space without corrupting what has already been learned at more distant points in the input space.

Our approach to neural network-based control utilizes network architectures suitable for on-line learning. Our recent work has indicated that shifts in control between the rule-based and neural network components of Fig. III-2 can be accomplished on-line using the fast learning capabilities of CMAC neural networks. It was shown that the use of B-Spline receptive field functions enables higher-order CMAC neural networks [10] to be constructed that can learn both functions and function derivatives. This ability coupled with the computational efficiency of CMAC neural networks allows on-line construction of multi-dimensional functions and their Jacobian matrices for use in inverse kinematics and dynamics transformations and reinforcement learning.

Multi-layer perceptron neural networks [11] are often slow to learn nonlinear functions with complex local structure due to the global nature of their function approximations. Neural networks based on local approximations, such as CMACs, are capable of learning nonlinear functions with localized structure quickly, but may generalize poorly and can require basis set sizes that scale exponentially with the dimension of the input space. We have shown that CMAC neural networks with B-Spline receptive field functions can be incorporated into the node connection functions computed in multi-layer perceptrons [12]. This allows Spline Net architectures to be

developed that are also suitable for on-line learning by combining the generalization capabilities and scaling properties of global multi-layer feedforward networks with the computational efficiency and learning speed of local network paradigms

b. Neural network training paradigms

In our approach to intelligent robotic control, many of the system components in Fig.II-3 are decomposed into feedback and neural network subsystems as shown in Fig. III-4. The output of the feedback and neural network subsystems, $\boldsymbol{u}^{fb}$ and $\boldsymbol{u}^{nn}$, respectively, are summed to obtain the total control command, **u**. $\mathbf{x}^d$ is the vector of desired states, and **x** is the vector of actual state values. As the neural network-based subsystem is trained, the feedback control law contribution, $\boldsymbol{u}^{fb}$, is driven to zero, and in the process, the neural network-based component learns the inverse dynamics of the system (in the sense that it can compute the required control command for a desired change in the system output). When the desired state values, $\mathbf{x}^d$, are used as network inputs instead of actual state values, **x**, system operation can be smoothly shifted from a predominantly feedback form of control to a predominantly feedforward form. The neural network component, $\boldsymbol{u}^{nn}$, is trained using a quadratic cost function of $\boldsymbol{u}^{fb}$ (or a differenced version $[\boldsymbol{u}^{fb}]_k - [\boldsymbol{u}^{fb}]_{k-1}$) to minimize the feedback component's contribution to the total control command, **u**. The *k* subscript represents the value of the control variables at time, t_k. This learning paradigm is commonly referred to in the literature as Feedback-Error-Learning [10].Reinforcement learning optimization is used to refine "rough-cut" task execution produced by constant coefficient motor synergies and primitive (untrained) joint servo-reflexes. This is done by first training the neural networks at the joint reflex level to represent the inverse dynamics of the system. When this phase of learning is completed, central pattern generator (CPG) neural networks [13,14] residing at the motor synergy level of the controller are trained to modulate the synergy strength coefficients as a function of time and/or the desired system state in order to minimize the amount of energy expended or the rate-of-change of torque applied. Minimization of the quadratic cost functions associated with energy or rate-of-change of torque requires solving a two-point boundary value problem due to the split boundary conditions on the state and adjoint equations. As a result, the reinforcement learning optimization utilizes a sweep method [15] to iteratively solve for the optimal synergy strengths. The forward sweep is accomplished as a maneuver is performed by storing a trace of the relevant system variables in a short-term memory buffer. Once it has been determined that the maneuver has ended, the system "thinks" about what it has just done by sweeping the adjoint sys-

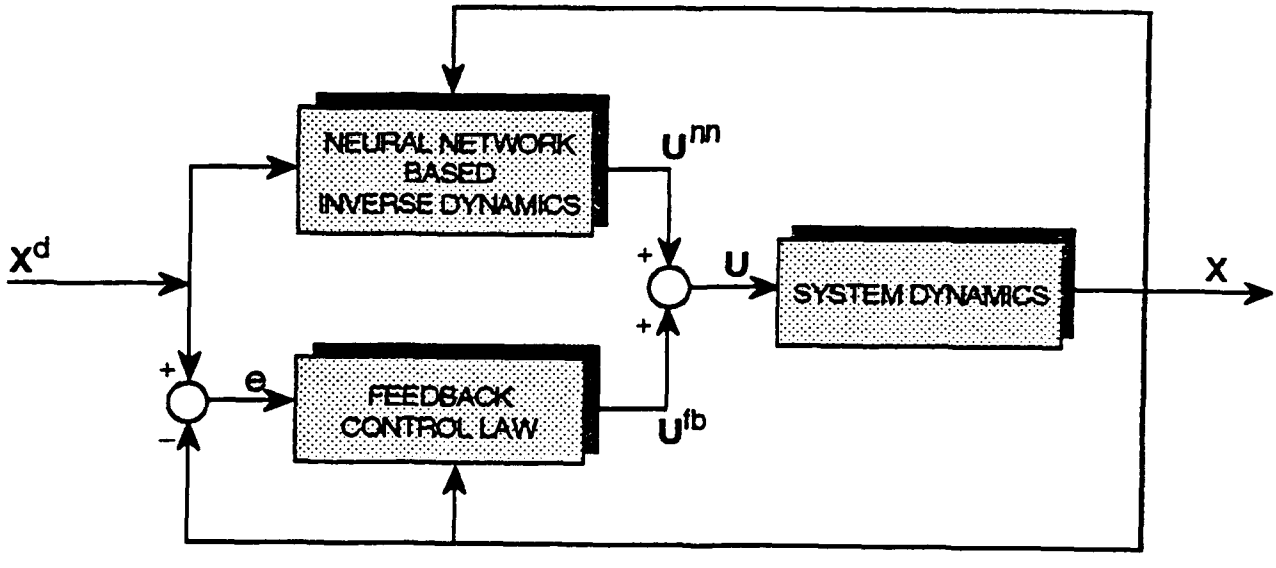

Figure III-4. Neural network control based on feedback-error-learning.

tem of equations backwards in time in order to make the next repetition of the maneuver closer to optimal. Since derivatives of the neural network-based joint reflexes are required in the reinforcement learning optimization, differentiable neural networks capable of local function approximation such as SplineNets [12] or BMACs [9] are used. The advantage of using recurrent networks such as Jordan Nets [14] to implement central pattern generators is that the synergy strengths can be modulated as either periodic or non-periodic functions of time. If feedforward networks such as BMACs [9] or Splinets are used, then the synergy strength coefficients will be modulated in a chained response fashion [13,16,17] based on the current value of the manipulator state. In either case, the use of central pattern generator neural networks allows the optimal maneuvers learned through practice to be generalized across space and time.

c. Learning automatic behaviors in multi-sensory robotic systems

One example of a multi-sensory integrated approach to robotic systems is presented in this report. A more complete discussion of these systems and other examples are given in Gelfand et al. [18]. Automatic control of a sensory-motor task is acquired through practice in an integrated system that uses visual input to execute a task and train a control system to perform that task using sensory inputs from joint position sensors.

A schematic diagram of a multisensory learning and control system is shown in Fig. III-5. A

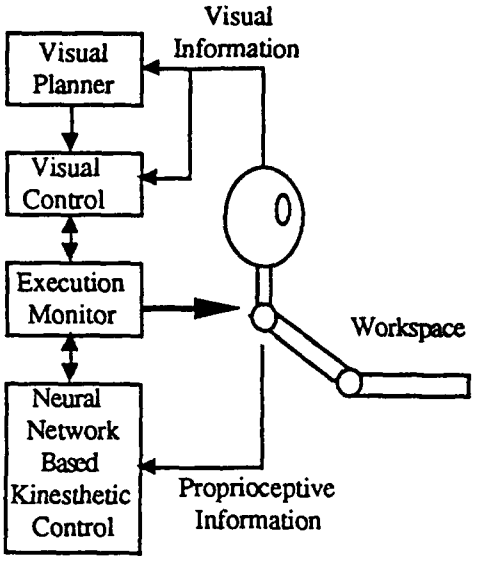

Figure III-5. A schematic diagram of a hybrid learning and control system. This system plans and executes the motion of an arm using visual input and trains the arm to perform the task using feedback from position sensors in the actuators.

simulated robot manipulator performs a task with a machine vision system initially determining the appropriate trajectory of the manipulator based on relevant information about the work space. This visual information is fed to the modules marked visual planner and visual control. The visual control module uses the visual feedback of the position of the arm to execute movement along the planned path. During the execution of this visually guided motion, proprioceptive sensors provide information about the arm's state to a CMAC neural network [19]. This network is trained to provide the proper control outputs to cause the arm to move in the same path as under visual system control. This CMAC controller provides a direct coupling from proprioceptive input to motor output for only that portion of trajectory space in which the response was learned in performing the task. The process described above is supervised by an execution monitor responsible for monitoring the performance of the kinesthetic control system relative to the visually controlled system and for switching control between them. The execution monitor also monitors the

gross performance of the system. If problems are encountered, such as an unexpected collision, control may be switched back to the visual system, which with its visual sensing of the whole workspace and general algorithmic controller allows for comprehensive diagnostics and possible retraining.

d. Learning control of an arm in the presence of an obstacle

In this demonstration, we use a visual system to locate an object in two-dimensional space and to control the motion of the two link manipulator. As shown in Figs. III-6a and 6b, a CMAC was trained to control the position of the manipulator as a function of measured joint angles. During the training passes, the RMS difference between the visually controlled manipulator position and the position suggested by the CMAC is monitored and used to determine when the CMAC has adequately learned the desired trajectory. The execution monitor then switches control from visually guided motion to kinesthetically controlled motion.

Referring to Fig. III-5, we see a two-link manipulator constrained to a horizontal plane. The arrangement of the manipulator, the object, and the visual system are shown. For the sake of this demonstration we used a simple binocular visual system that locates the object in space using the angles from the object to the sensors. The path was calculated by first determining a point of closest allowable approach based on the size of the end effector. This point and the given initial and final end effector positions were used to compute a spline function representing a desired trajectory. The visual system monitors the position of the end effector as the motion is controlled by torques calculated by the inverse dynamics of the arm. As the arm moves, the CMAC is given as input the current joint angles, joint velocities, and desired joint angles at the end of the segment. The CMAC is trained to output the required torques at each joint to produce the desired end effector trajectory. The training consists of comparing the torque output of the inverse dynamic controller with that of the CMAC and training the weights by the standard CMAC learning algorithm [19]. When the error falls below a predetermined level, control is switched from visual input based on end effector position to the CMAC.

The results of this demonstration are shown in Figs. III-6a am 6b. These figures depict the behavior of the system after the indicated number of runs. Each training run consists of a complete sweep of the trajectory from the initial position to the final position. In each figure, we use a thin line to indicate the actual trajectory of the end effector as controlled by the visual input con-

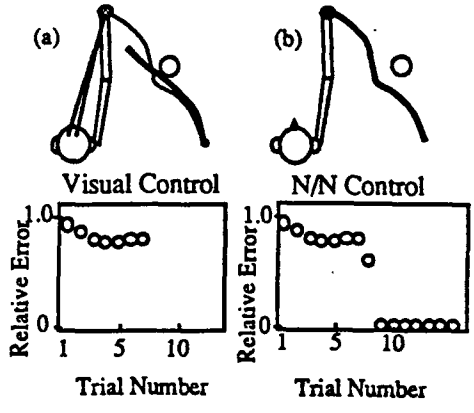

Figure III-6a and 6b. View from above the robotic arm under visual control training a CMAC neural network to execute the same trajectory using joint angle feedback. The graph at the bottom of each figure depicts the RMS difference between the visual and CMAC control as discussed in the text. In (a), the arm in its seventh sweep and control remains under the visual system. In (b), control of the arm has been transferred to the CMAC.

troller. The heavy lines indicate the motion that would result from using the commands from the CMAC controller. At the bottom of each figure, we show the RMS differences of the joint angles between the CMAC-controlled and visually control trajectories plotted against the number of training runs. In Fig. 6a, the lines from the robot's binocular visual sensors to the end effector indicate that the system is under visual control. We can see that the output of the CMAC begins to approach the desired path. The RMS difference becomes smaller and the trajectories depicted by the thin and heavy lines become coincident. In Fig. III-6b, we show the performance of the system after control has been transferred to the CMAC.

3. Task 3

Our hybrid rule-based/neural network control technique was initially used to integrate knowledge-based system and neural network techniques for the control of a two-link manipulator. A simulation was constructed in which a neural network learned how to perform a tennis-like manipulator swing. The control system utilized rule-based components to initiate the swinging maneuver and train the neural network. It was shown that for the manipulative task investigated, shifts between declarative and reflexive processing occurred smoothly, with no stability problems, and could be traced by variations in the number of rules being tested and the network output errors during learning. Additionally, real-time performance on economical hardware was indicated.

This control approach has subsequently been applied successfully (in simulation) to the control of the redundant six-link anthropomorphic robot shown in Fig.III-7 [21]

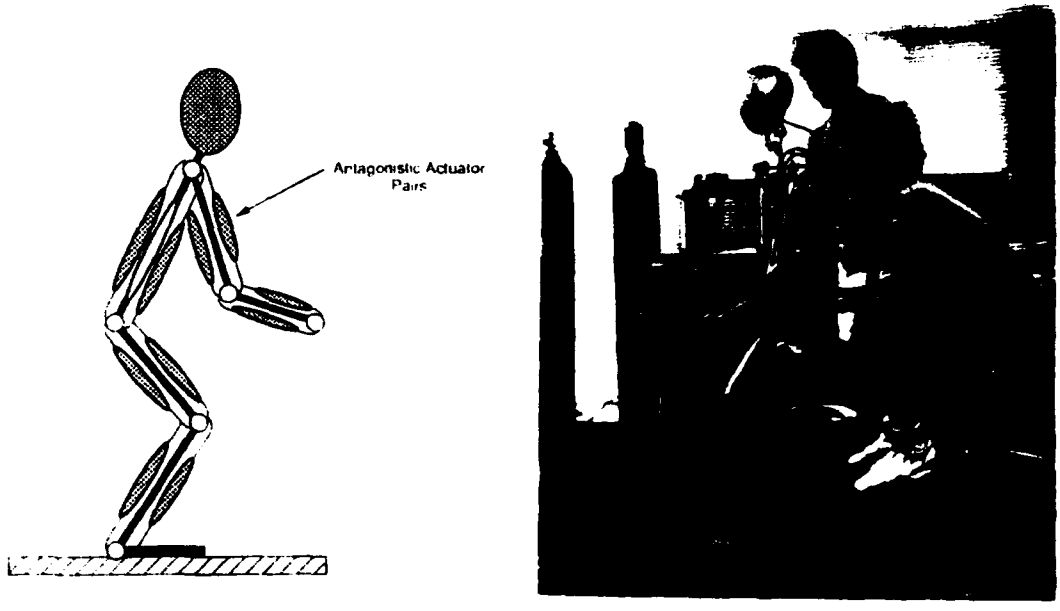

Figure III-7. SLIM, a planar, six-link, five-joint robot that "stands" six-feet tall.

In addition to simulation, we have also begun to implement aspects of the hybrid architecture to a physical version of SLIM (Skill Learning Intelligent Manipulator). Here, we describe the hardware and its current level of functioning. It is important to recognize that the hardware lags our simulations because of the non-ideal behavior of the structure and the actuators.

SLIM is a planar, six-link, five-joint robot that "stands" roughly six-feet tall. The robot looks like a person in profile. It is made of light-weight aluminum I-beams that are hinged at the joints using ball bearings. Each joint is controlled by a pair of soft pneumatic actuators known as rubbertuators. These rubbertuators are antagonistically arranged and each can develop about 350

lbs. of force. The rubbertuators are made by the Bridgestone Corporation of Japan. The artificial muscles are driven by proportional control valves that serve the pressure in each muscle to a value determined by the control software. The force in each muscle is sensed by a load cell, and the joint angles are sensed by linear potentiometers.

Two IBM-compatible 386/33 MHz computers are used to implement the control algorithm and display the state of the manipulator. The two computers are linked by a high bandwidth fiber-optic data link. One computer uses a PID control based on angle to get SLIM to achieve a desired posture as determined by program running on the other computer. The posture-determining algorithm is a modified Berkinblitt approach that is a forward approximation solution to the inverse kinematics of the link-redundant robot [22]. The algorithm is modified to improve convergence by inclusion of low-level muscle synergies (reflexes) that allow the coordinated withdrawal or extension of the arm or leg. Without these synergies, each joint acts separately, and motions such as limb extension or withdrawal proceed slowly. With these elements (posture controller and joint angle PID controller), we have gotten SLIM to stand and exercise free motion by tracking his end-point (end of arm) along a line of arbitrary inclination, or along a circle.

We have also added active joint compliance control so that any joint of the robot can be stiffened or loosened at will. Recall that SLIM is a compliant structure, so that, in response to external push, he will give way to a degree determined by the joint compliance. Recently, we have added a CMAC network to improve the tracking ability of the PID controller for one joint of the robot. The CMAC is necessary because the rubbertuators are non-linear so that PID gains must vary for different postures to obtain optimal and stable performance. The CMAC feed-forward controller learns to compensate so that knee position error is reduced. In essence, the CMAC is learning the inverse dynamics about a given joint angle and the information is used to create a better controller. The learning method here is due to Kawato, and its trains the CMAC to drive the feedback component to zero. We are presently generalizing this result to other joints of the robot.

To deal with computing limitations, we have also developed a new Digital Signal Processor (DSP) architecture and have begun to implement it on SLIM. The architecture involves the use of both shared and global memory and has a low-speed ascending and descending data bus in analogy with the ascending and descending pathway in the human spinal cord.

D. PUBLICATIONS

1. Handelman, D. A., S. H. Lane, and J. J. Gelfand, "Integrating Neural Networks and Knowledge-Based Systems for Intelligent Robotic Control," *IEEE Control Systems Magazine*, April 1990, pp. 77-87.
2. Lane, S. H., D. A. Handelman, and J. J. Gelfand, "Can Robots Learn Like People Do?" *Proc. of the SPIE Conf. on Applications of Artificial Neural Networks*, Orlando, FL., April 1990.
3. Lane, S. H., D. A. Handelman, and J. J. Gelfand, "Reinforcement Learning and Optimization in Intelligent Robotic Control Systems," *Presented at 5th IEEE Symposium on Intelligent Control*, Philadelphia, Sept. 1990.
4. Handelman, D. A., S. H. Lane, and J. J. Gelfand, "Focusing Attention Within Adaptive Hybrid Controller Hierarchies for Robotic Skill Acquisition," *Proceedings of the 5th IEEE Symposium on Intelligent Control*, Philadelphia, Sept. 1990.
5. Lane, S. H., D. A. Handelman, J. J.Gelfand, and M. Flax, "Function Approximation Using Multi-Layered Neural Networks and B-Spline Receptive Fields," *Advances in Neural Information Processing Systems*, **3**, D. Touretzky, Ed., Morgan Kaufmann, Palo Alto, 1991, p. 684-693.
6. Lane, S. H., D. A. Handelman, and J. J. Gelfand, "An Architecture for Robotic Skill Acquisition Incorporating Structural and Functional Aspects of the Human Motor Control System," *Submitted to IEEE Expert*, 1991.

7. Handelman, D. A., S. H. Lane, and J.J. Gelfand, "Goal-Directed Encoding of Task Knowledge for Robotic Skill Acquisition," *Proceedings of the Sixth IEEE International Symposium on Intelligent Control, Arlington, Va., August, 1991, IEEE Press,* New York (1991) p. 388-393.
8. Lane, S. H., D. A. Handelman, and J. J. Gelfand, "Higher-Order CMAC Neural Networks - Theory and Practice," *Proceedings of the 1991 IEEE American Control Conference, Boston, MA, June 1991, IEEE Press*, New York, 1991.
9. Lane, S. H., D. A. Handelman, and J. J. Gelfand, "Theory and Development of Higher-Order CMAC Neural Networks," *IEEE Control Systems Magazine*, April 1992.
10. Gelfand, J. J., M. Flax, R. Endres, S. H. Lane, and D. A. Handelman, "Acquisition of Automatic Activity Through Practice: Changes in Sensory Input," *Proceedings of Tenth National Conference on Artificial Intelligence*, San Jose, July 1992, AAAI Press, Menlo Park, (1992) p. 189-193.
11. Lane, S. H., D. A. Handelman, and J. Gelfand, "Modulation of Robotic Motor Synergies Using Reinforcement Learning Optimization," Bekey, G. and Goldberg, K, Eds., *Neural Networks in Robotics*, Kluwer Academic Pub., Norwell, MA, 1992, p. 521-538.
12. Gelfand, J. J., M. Flax, R. Endres, S. H. Lane, and D. A.Handelman, "Senses, Skills, Reactions and Reflexes: Learning Automatic Behaviors in Multi-Sensory Robotic Systems," Bekey, G., and Goldberg, K., Eds., *Neural Networks in Robotics*, Kluwer Academic Pub., Norwell, MA, 1992.
13. Handelman, D. A., S. H. Lane, and J. J. Gelfand, "Robotic Skill Acquisition Based on Biological Principles," Kandel, A. & Langholz, G., Eds., *Hybrid Architectures for Intelligent Systems*, CRC Press, Boca Raton, FL, 1992, p. 301-328.

E. REFERENCES

1. Fitts, P. and M. Posner, "Human Performance," (Brooks/Cole Pub. Co., Belmont, CA, 1967), p. 8.
2. Kupfermann, I., "Learning," *Principles of Neural Science*, edited by E. Kandel and J. Schwartz, (Elsevier Science Pub. Co., New York, 1985), p. 810.
3. Bizzi, E., N. Accornero, W. Chapple, and N. Hogan, "Posture control and trajectory formation during arm movement," *Journal of Neuroscience*, **4,** 2738-2745, (1984).
4. Brooks, V., "The Neural Basis of Motor Control," *Oxford University Press,* New York, (1986).
5. Posner, M. I., M. J. Nissen, and R. M. Klein, "Visual Dominance: an Information Processing Account of its Origin," *Psychology Review*, **83,** 157-171 (1976).
6. Notterman, J. M., and D. O. Weitzman, "Organization and Learning of Visual-Motor Information During Different Orders of Limb Movement: Step, Velocity, Acceleration," *J. Exp. Psych.: Human Perception and Performance*, **7**, 916-927 (1981).
7. Fischman, M. G. and T. Schneider, (1985). "Skill Level, Vision, and Proprioception in Simple One Hand Catching," *J. Mot. Behavior*, **17,** 219-229.
8. Schneider, W. and Fisk, A., "Attention Theory and Mechanisms for Skilled Performance," in Magill, R., Ed., *Memory and The Control of Action*, North-Holland Publishing, Amsterdam, 119-143 (1983).
9. Lane, S. H., D. A. Handelman, and J. J. Gelfand, "Higher-order CMAC Neural Networks - Theory and Practice," *Proc. 1991 American Control Conf.*, Boston, June 1991.
10. Miyamoto., M. Kawato, T. Setoyama, and R. Suzuki, "Feedback-Error-Learning Neural Network for Trajectory Control of a Robotic Manipulator," *Neural Networks,* **1,** 251-265, (1988).

11. Rumelhart, D. E., and J. L. McClelland, "Parallel Distributed Processing - Explorations in the Microstructure of Cognition," *MIT Press*, Cambridge, MA (1986).
12. Lane, S. H., D. A. Handelman, and J. J. Gelfand, "Multi-layer Perceptrons With B-Spline Receptive Field Functions," *Presented at Neural Information Processing Systems Conf.*, Denver, Nov. 1990.
13. Gallistel, C.R., "The Organization of Action," Lawrence Erlbaum Assoc., Hillsdale, New Jersey, 1980.
14. Jordan, M.I., "Attractor Dynamics and Parallelism in a Connectionist Sequential Machine," *Proc. 8th Annual Conf. Cognitive Science Society,* 1986, pp.531-546.
15. Stengel, R. F., "Stochastic Optimal Control: Theory and Applications," John Wiley & Sons, New York, (1986).
16. Easton, T.A., "On the Normal Use of Reflexes," American Scientist, **60,** Sept.-Oct. 1972, pp. 591-599.
17. Greene, P.H., "Problems of Organization of Motor Systems," Progress in Theoretical Biology, R. Rosen and F.M. Snell, *Eds. Academic Press*, New York, 1972.
18. Gelfand, J., Flax, M., R. Endres, S. Lane and D. Handelman, "Acquisition of Automatic Activity Through Practice: Changes in Sensory Input", *Proceedings, Tenth National Conference on Artificial Intelligence*, San Jose, July 1992, AAAI Press, Menlo Park (1992) p. 189-193.
19. Albus, J., "A New Approach to Manipulator Control: The Cerebellar Model Articulation Controller" (CMAC), J. Dyn. Syst. Meas. and Cont., **97**, 270-277 (1975).
20. Handelman, D. A., S. H. Lane, and J. J. Gelfand, "Integrating Neural Networks and Knowl-Edge-based Systems for Intelligent Robotic Control," *IEEE Control Systems Magazine*, April 1990, pp. 77-87.
21. Lane, S. H., D. A. Handelman, and J. J. Gelfand, "Can Robots Learn Like People Do?" *Proc. of the SPIE Conf. on Applications of Artificial Neural Networks*, Orlando, FL, April 1990.
22. Berkinblitt, M.V., Gelfand, I.M., and Feldman, A.G., "Model of the Control of the Movements of a Multi-joint Limb," *Biophysics*, **31**, (1), 1986, pp. 142-153.